

Electronic Supplementary Information

Visible light-driven molecular oxygen activation for oxidative amidation of alcohols using lead-free metal halide perovskite

Vishesh Kumar,^a Ved Vyas,^a Deepak Kumar,^a Ashish Kumar Kushwaha,^b and Arindam Indra^{*a}

^a*Department of Chemistry, Indian Institute of Technology (BHU), Varanasi, UP-221005, India*

E-mail: arindam.chy@iitbhu.ac.in

^b*Department of Chemistry, Banaras Hindu University, Varanasi, UP-221005, India*

Chemicals

All chemicals are of analytical grade and used without further purification.

Copper(II) bromide (99.9%), Cesium bromide, oleic acid (OA, 90%), Oleylamine (OAm, 90%), Dimethyl sulfoxide (DMSO) and 1-octadecene (ODE, 91%) were purchased from Sigma-Aldrich. Tetrabutylammonium hexafluorophosphate (TBAPF₆) was purchased from BLD Pharma. Ethyl acetate (CH₃COOC₂H₅, 99.9%), Hexane (99.9%), Tetrahydrofuran (THF), acetonitrile, toluene, isopropanol (IPA), Methanol, Ethanol, and dimethyl sulfoxide (DMSO-d₆) were purchased from Merck. *P*-Nitro-Blue tetrazolium chloride (NBT) and *o*-tolidine were purchased from Sigma-Aldrich. Chloroform-d (CDCl₃), and silica gel were purchased from Merck. All aldehydes and amine substrates were purchased from either Sigma-Aldrich, SRL, Merck, or Avra Chemicals.

Instruments

The crystal structure of the catalysts was confirmed by High-resolution X-ray diffractions (HR-XRD) carried out in the Rigaku Smart Lab 9kW Powder X-ray diffractometer (RIGAKU Corporation). Scanning Electron Microscopy (FE-SEM) studies were carried out in Nova Nano SEM 450, FEI Company of USA (S.E.A.) PTE, LTD. Energy dispersive X-ray spectroscopy (EDX) images were collected by Team Pegasus Integrated EDS-EBSD with Octane Plus and Hikari Pro EDX System. Elemental mapping was performed with the analyzer attached to SEM. TEM studies were carried out on a Tecnai G2 20 TWIN transmission electron microscope connected with an energy-dispersive X-ray spectrometer (EDAX, r-TEM SUTW).

The X-ray photoelectron spectroscopy (XPS) measurements were performed in a K-Alpha X-ray photoelectron spectrometer from Thermo Fisher Scientific. The binding energies were calibrated using the C 1s peak at 284.6 eV as the reference.

Diffuse reflectance spectroscopy (DRS) measurements using UV-Vis. spectroscopy was conducted utilizing an AvaSpec-ULS2048L instrument. Photoluminescence was acquired on a TCSPC system from Horiba Yovin (Delta Flex).

^1H -NMR spectra were recorded on AVH D 500 AVANCE III HD 500 MHz NMR Spectrometer from Bruker Bio Spin International. The Chemical shifts were reported in ppm. Coupling constants are expressed in Hertz (Hz). The following abbreviations are used: s = singlet, bs = broad singlet d = doublet, t = triplet, and m = multiple. The residual solvent signals were used as references for ^1H and ^{13}C NMR spectra (CDCl_3 : $\delta_{\text{H}} = 7.28\text{-}7.29$ ppm, $\delta_{\text{C}} = 77.01\text{-}77.16$ ppm).

HRMS (m/z) were recorded in an electron ionization or electrospray ionization (ESI) mode on Waters-Q-TOF Premier-HAB213 and Sciex X500R QTOF instruments.

Light source: (JACKAL, LED 3-Watt blue light, 460 nm). 5 Lights were used together.

Experimental

Synthesis of Cs_2CuBr_4 by hot injection method (PC-1)

Initially, a Cs-OA precursor stock solution was prepared by adding Cs_2CO_3 (203 mg), ODE (10 mL), and OA (0.5 mL) in a 50 mL three-neck flask, heated at 120 °C for 1 hour under an N_2 atmosphere. Subsequently, CuBr_2 (1 mmol), ODE (10.0 mL), OAm (1.0 mL), and OA (1.0 mL) were introduced into a 25 mL three-neck flask and dried at 120 °C for 1 hour under an N_2 atmosphere. The temperature was then raised to 170 °C, and the Cs-OA stock solution (0.5 mL) was rapidly injected and stirred for 1 minute to attain complete solubility. The resulting reaction mixture was promptly cooled down by placing the flask in an ice-water bath. The precipitate was isolated via centrifugation, washed with acetone, and dispersed in toluene for subsequent utilization and named PC-1.¹

Synthesis of Cs_2CuBr_4 at room temperature (PC-2)

Cs_2CuBr_4 was prepared by dissolving 212 mg of CsBr (1.0 mmol) and 111.67 mg of CuBr_2 (0.5 mmol) in 20 mL of DMSO to create a homogeneous precursor solution. This solution was introduced into 50 mL of isopropanol under vigorous stirring, leading to the completion of the reaction within 1 minute. Further centrifugation at 10000 rpm for 5 minutes to obtain the final product named PC-2.²

The PC-2 particle size varies with the amount of isopropanol, which is crucial because it initiates both nucleation and particle growth. However, increasing the amount of isopropanol leads to smaller particle sizes due to slower nucleation, with the synthesis temperature maintained at $35\pm 2^\circ\text{C}$.

Table S1. Description of the catalysts

S.N.	Photocatalyst	Synthesis methods	Catalyst named
1	Cs ₂ CuBr ₄	Hot-injection	PC-1
2	Cs ₂ CuBr ₄	Room temperature	PC-2

Photoelectrochemical Experiments. Photoelectrochemical measurements including photocurrent response and electrochemical impedance spectra (EIS) and Mott–Schottky analyses were conducted using a (Metrohm Auto Lab M204 workstation). The setup included a Pt wire as the counter electrode, Ag/AgCl as the reference electrode, and the working electrode composed of FTO loaded with the sample. Tetrabutylammonium hexafluorophosphate (0.1M TBAPF₆) in ethyl acetate or acetonitrile was used as electrolyte.

The working electrodes were prepared using Cs₂CuBr₄. The Fluorine-doped titanium oxide (FTO)-glass was first cleaned by ultrasonication in ethanol and then rinsed with deionized water and isopropyl alcohol (IPA). 3 mg catalyst was dispersed in 2 mL of toluene and sonicated for 10 min. A 50 μ L suspension was dropped onto 1 cm² of FTO and dried for about 40 min under an ambient atmosphere. The photocurrent test was measured vs Ag/AgCl bias potential under a blue LED visible light. EIS plots were recorded in the frequency range from 0.01 to 10⁶ Hz with an amplitude of 5 mV.

Figures

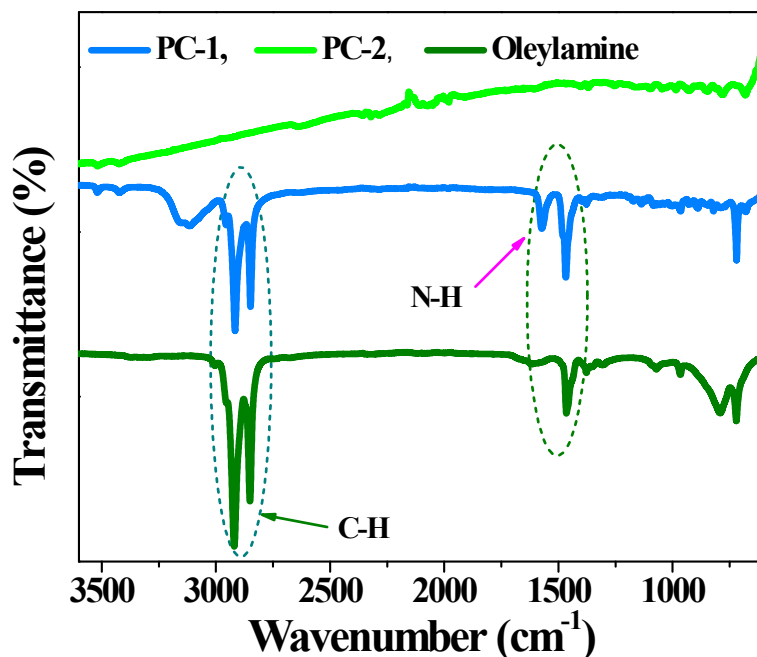


Figure S1. The FTIR spectra of pure oleylamine, PC-1, and PC-2. PC-1 shows the peaks for surface ligand oleylamine: Asymmetric in-plane stretching (CH₃) and methylene asymmetric C–H stretching (CH₂) appear at 2920 and 2849 cm⁻¹, respectively. The band at 1585 cm⁻¹ is due to -NH₂ scissoring. In the case of room-temperature synthesized PC-2, no surface ligand was present.

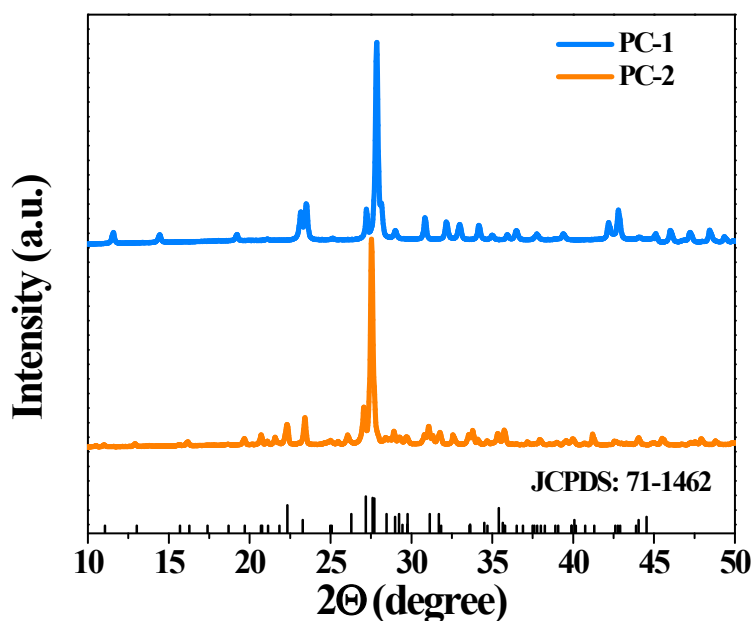


Figure S2. PXRD patterns of PC-1 and PC-2 matched with JCPDS no. 71-1462.

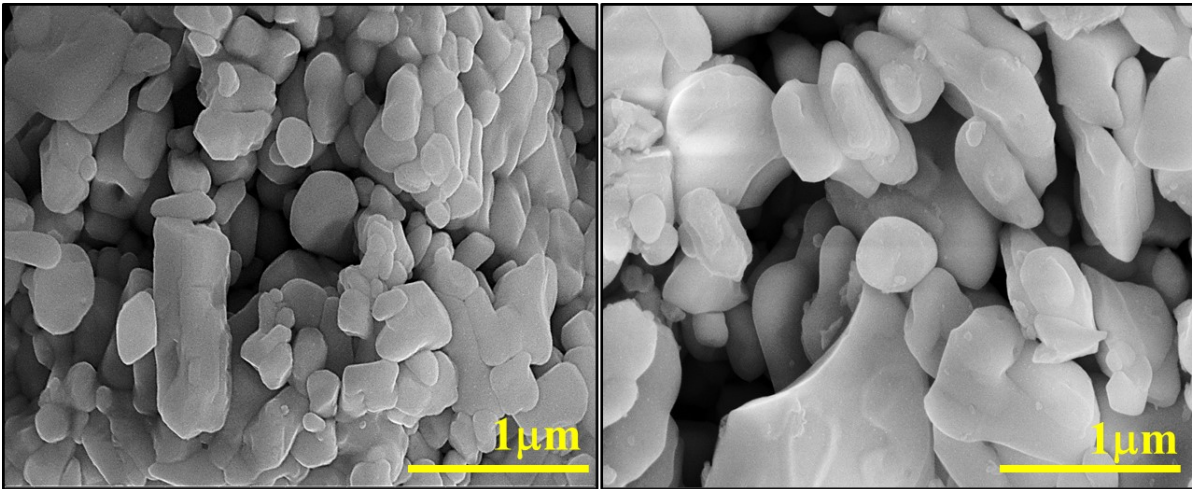


Figure S3. SEM images of PC-2 showing large and irregular-shape particles.

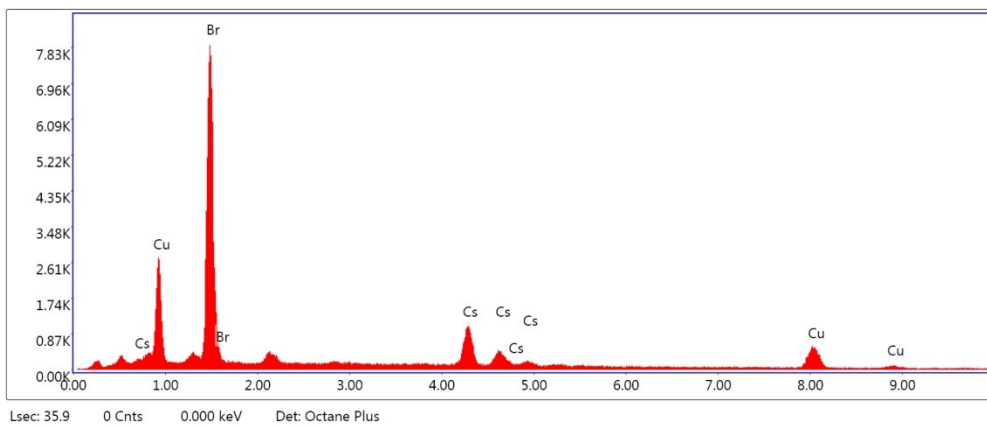


Figure S4. EDX spectrum of PC-1 showing Cs, Cu, and C.

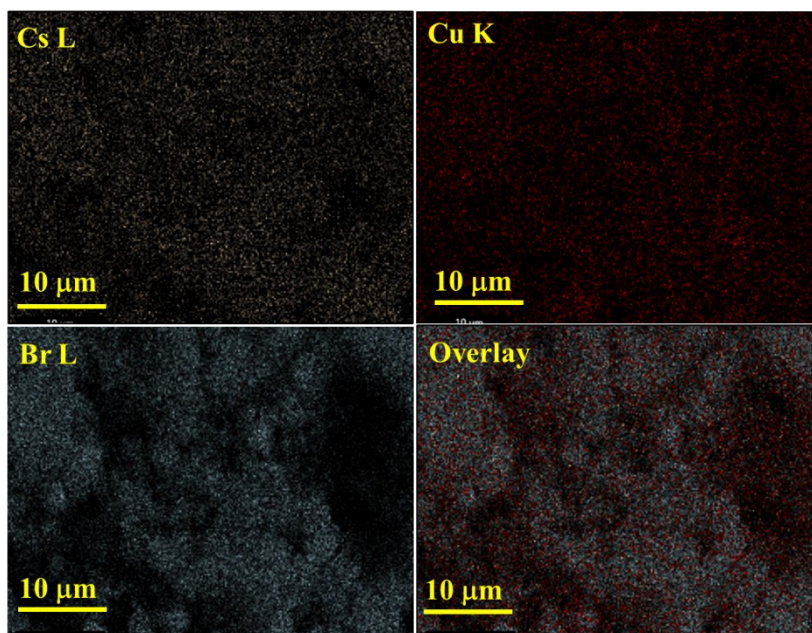


Figure S5. Elemental mapping of PC-1 showing the uniform distribution of Cs, Cu, and Br.

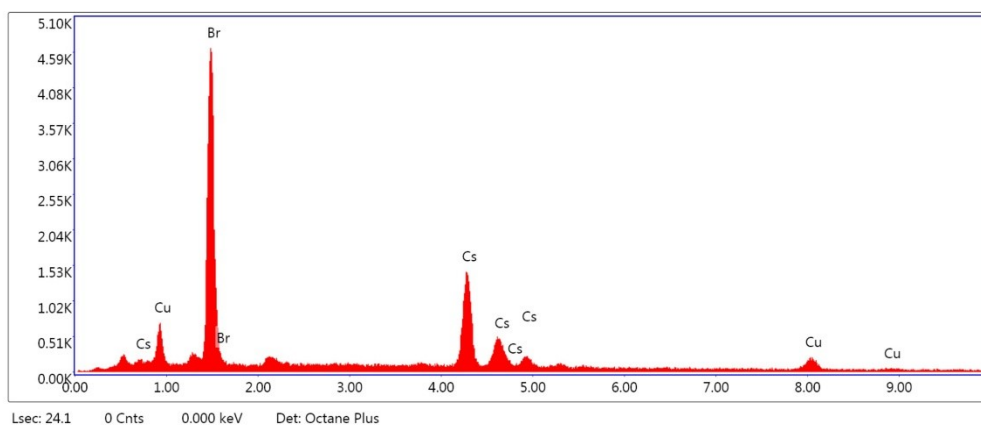


Figure S6. EDX spectrum of PC-2 showing Cs, Cu, and C.

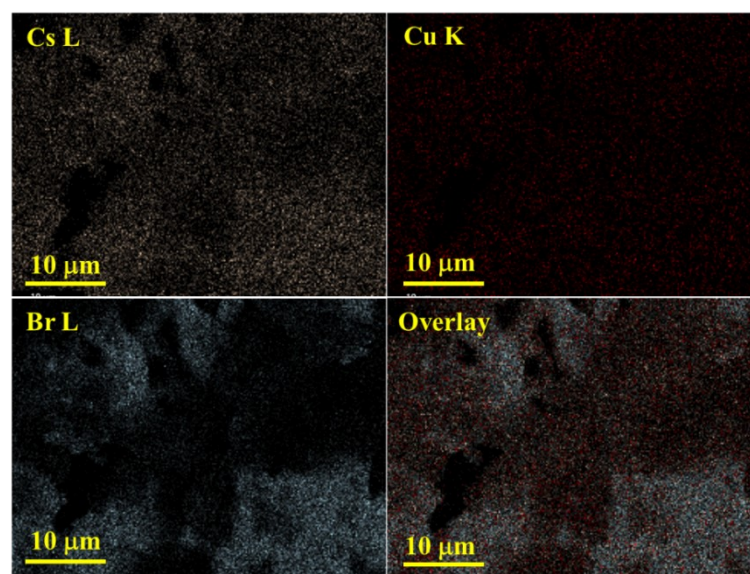


Figure S7. Elemental mapping of PC-2 showing the uniform distribution of Cs, Cu, and Br.

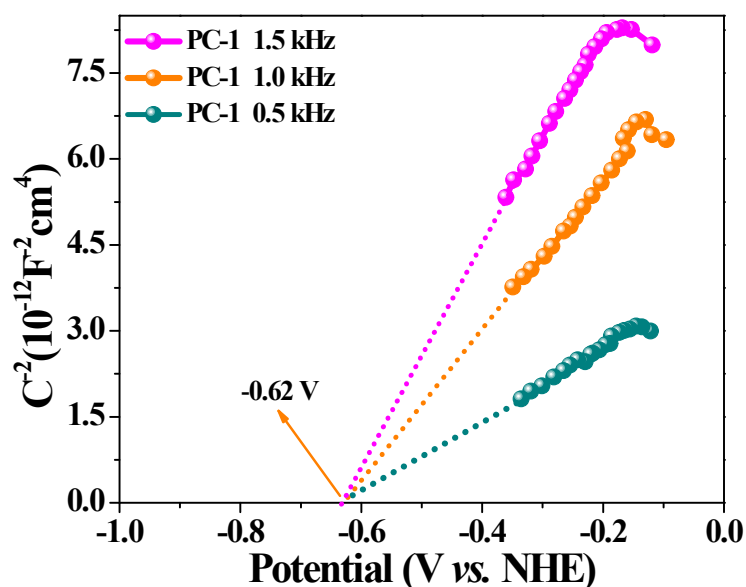


Figure S8. Mott-Schottky plot confirmed the conduction band position of PC-2. A Mott-Schottky plot determines the flat band potential (E_{fb}) and charge carrier densities. For n-type semiconductors, the conduction band minimum is about 0.1 to 0.2 V more negative than E_{fb} . The determination of the flat band potential involves the measurement the differential capacitance of the electric double layer at the semiconductor-electrolyte interface. The estimation of the flat band potential involves calculating the electron affinity (conduction band energy) on an absolute potential scale and assuming that the potential at flat band conditions lies between the conduction band edge and the valence band edge. The total capacitance includes contributions from semiconductor capacitance and the Helmholtz layer capacitance (C_H), typically 0.1 to 0.2 F/m² in a series.

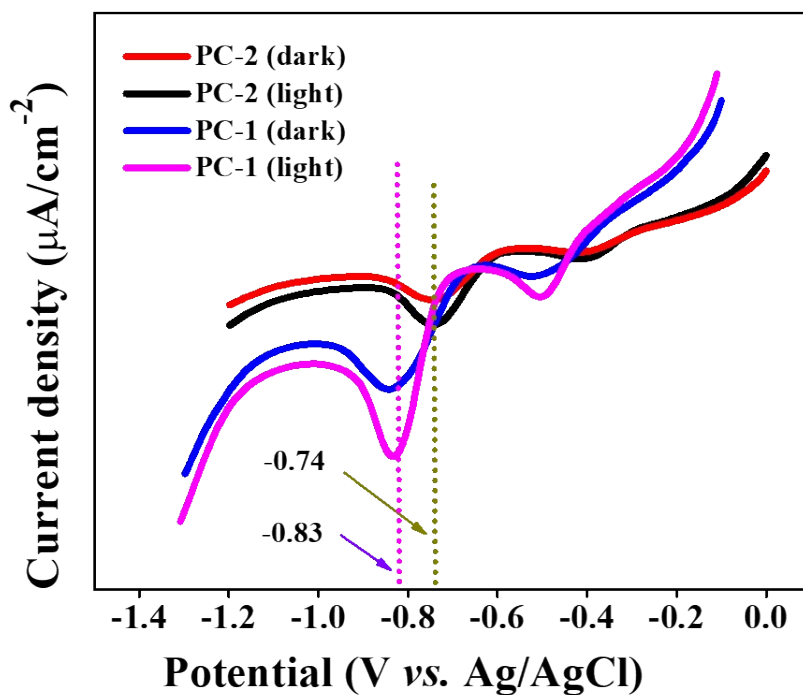
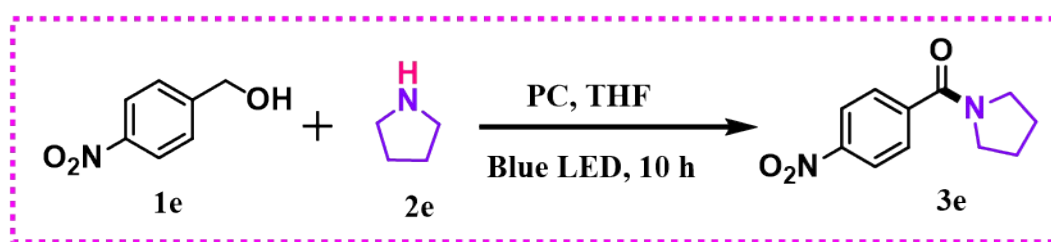


Figure S9. Differential pulse voltammograms (DPV) for PC-1 and PC-2 under dark and light. The experiments were conducted in a 0.1 M TBAPF₆ in acetonitrile solution at a scan rate of 10 mV s⁻¹.

Table S2. Optimization of the reaction conditions for photocatalytic amination of alcohols.



S.N.	Photocatalyst	Solvent	Conditions	Light	Time (h)	Yield (%)
Variation of catalysts						
1	PC-1	THF	air	Blue LED	10	97
2	PC-2	THF	air	Blue LED	10	74
Variation of solvents						
3	PC-1	Acetonitrile	air	Blue LED	10	67
4	PC-1	THF	air	Blue LED	10	97
5	PC-1	1,4-Dioxane	air	Blue LED	10	84
6	PC-1	Toluene	air	Blue LED	10	63
7	PC-1	Methanol	air	Blue LED	10	27
8	PC-1	Ethanol	air	Blue LED	10	22
9	PC-1	DMSO	air	Blue LED	10	58
Other variations in the reaction conditions						
10	-	THF	air	Blue LED	10	No Reaction
11	PC-1	THF	air	Dark	10	~ 4
12	PC-1	THF	N ₂	Blue LED	10	No Reaction
13	PC-1	THF	Pure O ₂	Blue LED	8	98

Reaction conditions: 10 mg PC-1 or PC-2, 4-nitrobenzyl alcohol (0.5 mmol), pyrrolidine (1.0 mmol), solvent (3 mL), air, time 10 h, 15 W blue LED at 35±2 °C temperature. The photocatalyst was separated from the reaction mixture by centrifugation at 13,000 rpm for 15 minutes. The product was separated by column chromatography in a silica column using different ratios of ethyl acetate and hexane as the eluent. ¹H and ¹³C NMR spectra were used to detect the formation and purity of the product. In all the cases, isolated yield of the product was reported.

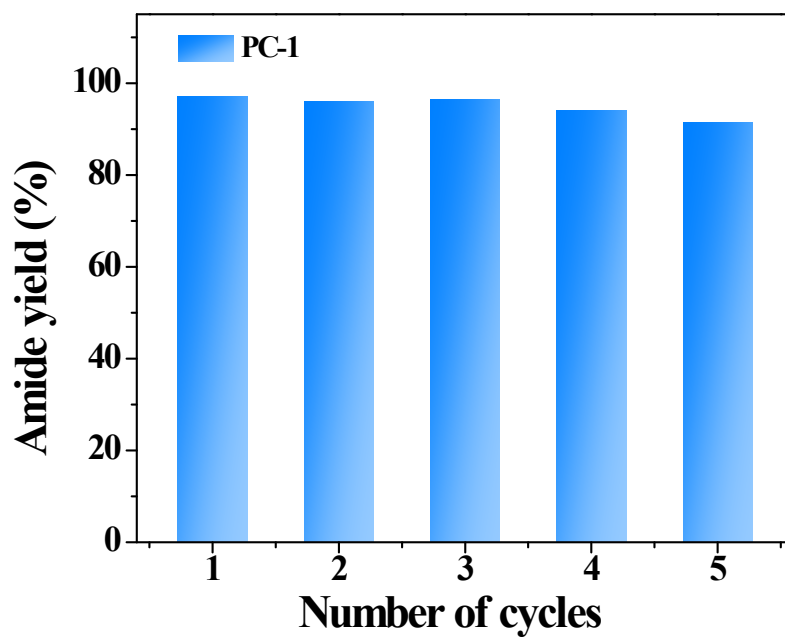


Figure S10. Recyclability of PC-1 photocatalyst for amide bond formation reaction.

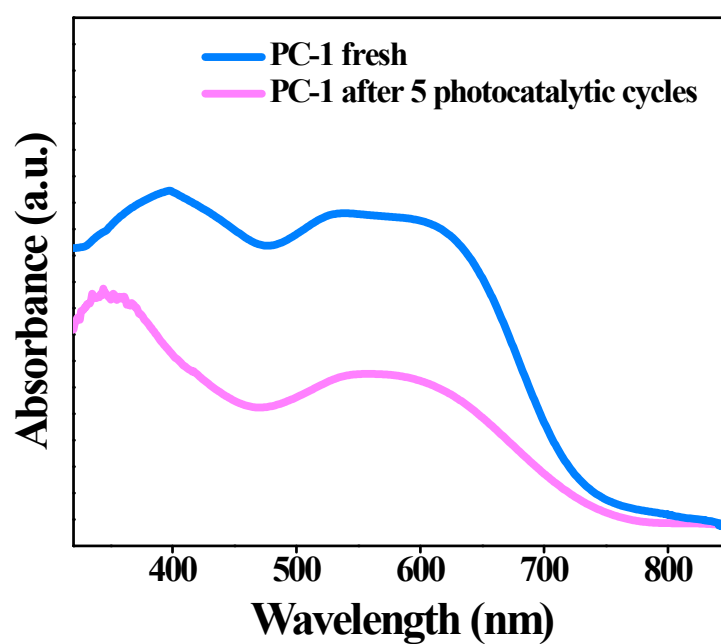


Figure S11. UV-vis-DRS of PC-1 after five cycles and before catalysis.

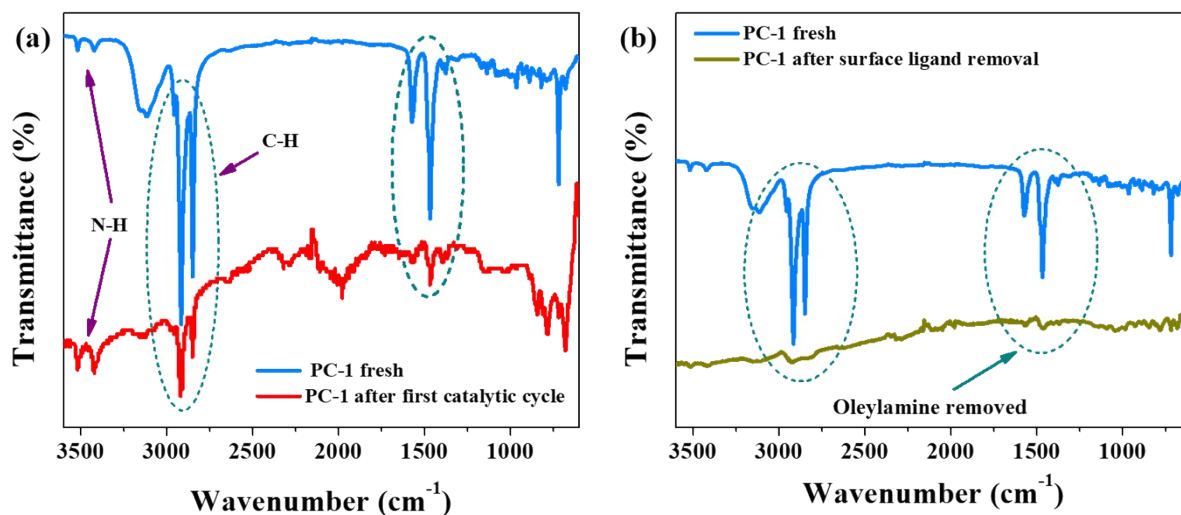


Figure S12. (a) FT-IR spectra of PC-1 after 1st cycle of photocatalysis show the remaining oleylamine ligand. (b) In contrast, after several times washing of PC-1 with ethyl acetate removes the surface ligand.

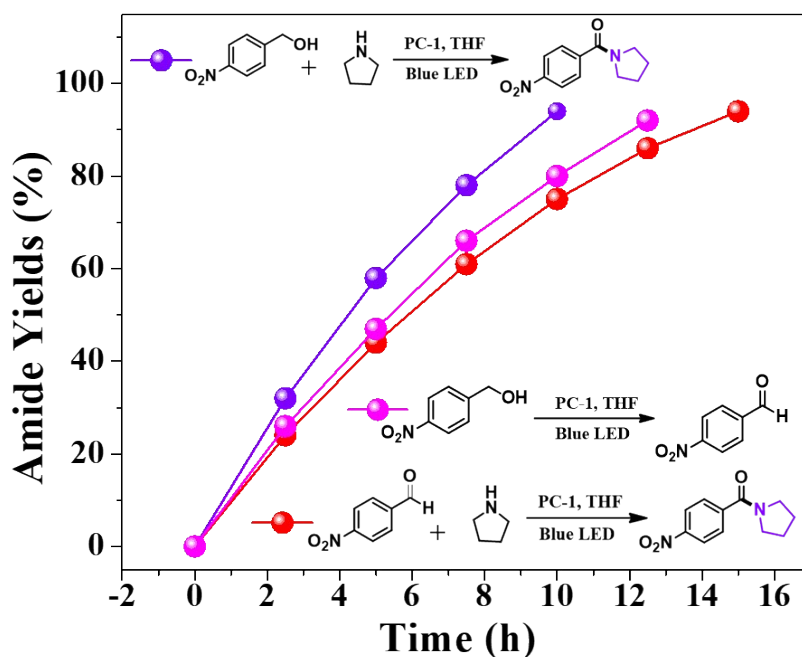


Figure S13. Difference in the rate of the reactions for C–N bond formation (a) 4-nitrobenzyl alcohol and pyrrolidine vs. (b) 4-nitrobenzaldehyde and pyrrolidine with PC-1. 4-nitrobenzyl alcohol (without amine) is converted into 4-nitrobenzaldehyde by photocatalytic oxidation.

The amide bond formation by C–N coupling can be achieved through two different routes: (a) direct coupling of benzyl alcohol and amine or (b) oxidation of benzyl alcohol to benzaldehyde and the reaction of benzaldehyde with amine. To clarify this point, we have conducted three different experiments by monitoring the product yield against time:

- (i) The reaction of 4-nitrobenzyl alcohol with pyrrolidine
- (ii) The reaction of 4-nitrobenzyl alcohol in the absence of any amines

(iii) The reaction of 4-nitrobenzaldehyde with pyrrolidine

In the reaction (i) and (iii) the corresponding amide was formed while reaction (ii) leads to the formation of 4-nitrobenzaldehyde. Therefore, it is clear that both 4-nitrobenzyl alcohol and 4-nitrobenzaldehyde can react with pyrrolidine to form the same amide. However, the reaction rate followed the order: (i) > (ii) > (iii)

The rate of the reactions showed that the photocatalytic reaction proceeds through the direct coupling of 4-nitrobenzyl alcohol and pyrrolidine instead of the conversion of 4-nitrobenzyl alcohol to 4-nitrobenzaldehyde and further its reaction with pyrrolidine. As the conversion rate of 4-nitrobenzyl alcohol to 4-nitrobenzaldehyde is slower than the coupling reaction (i), the possibility of reaction (iii) can be omitted in the present study.

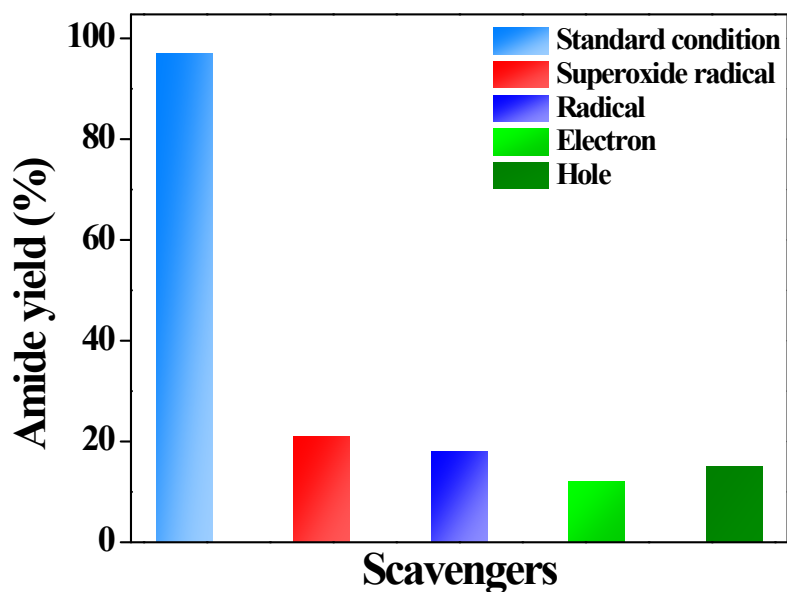


Figure S14. Quenching experiments confirmed the radical process involved in the amide bond formation reaction. *Para*-benzoquinone, TEMPO, AgNO₃, and triethylamine are used as the superoxide radicals, free radicals, electrons, and hole scavengers, respectively.

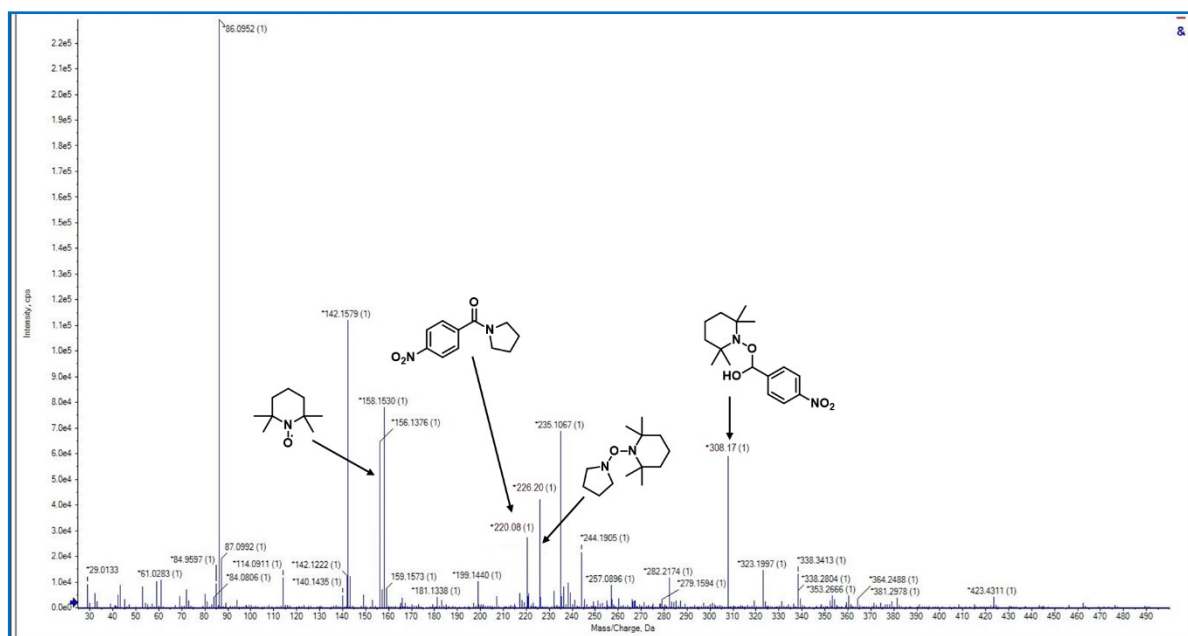
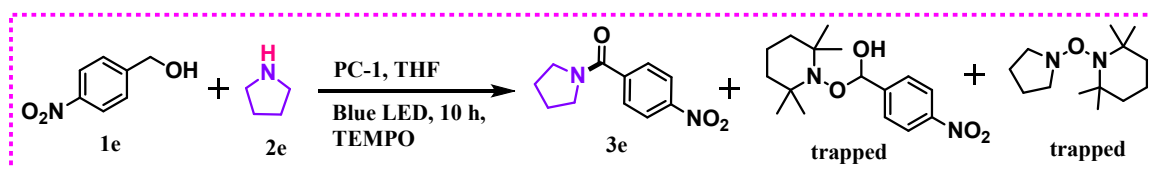


Figure S15: Mass spectrometry data of the reaction mixture detected the trapped intermediates and product (Radical trapping agent: 2,2,6,6-tetramethyl-1-piperidinyloxy, TEMPO).

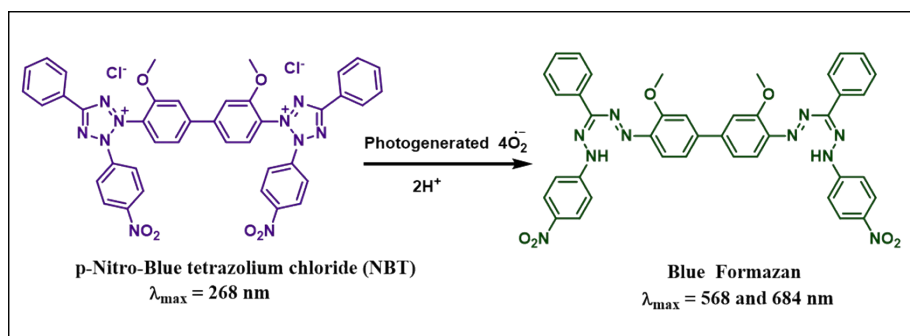
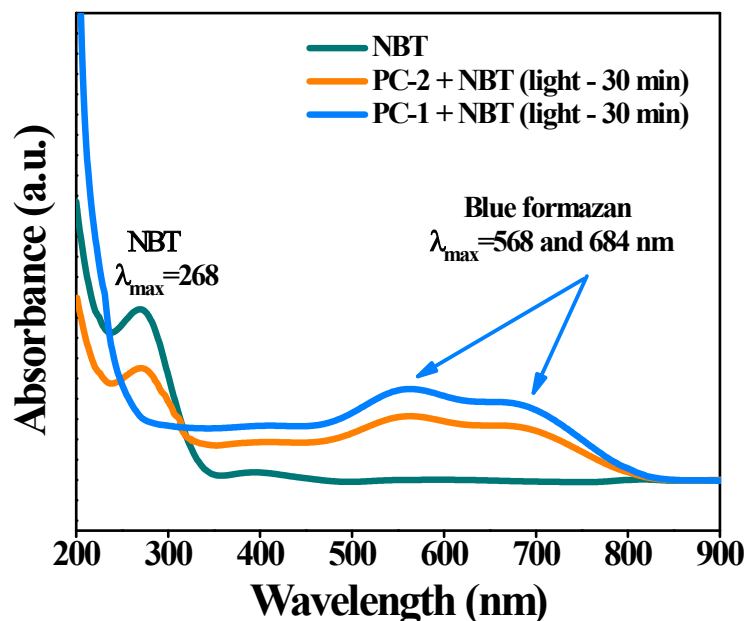


Figure S16. Detection of photogenerated superoxide radicals.

Reaction conditions: Photogenerated superoxide radical was detected using *p*-Nitro-Blue tetrazolium chloride (NBT) as an $\text{O}_2^{\bullet-}$ radical indicator. In the presence of $\text{O}_2^{\bullet-}$, NBT is reduced by electrons, forming blue formazan which shows strong UV-visible absorption signals at around 568 and 684 nm.³ As shown in Figure S14, two distinct absorption peaks can be found after irradiation to a 15W blue LED, indicating that PC-1 and PC-2 produce $\text{O}_2^{\bullet-}$ under light irradiation. This reaction validates the role of $\text{O}_2^{\bullet-}$ in driving photocatalytic amide bond formation via dehydrogenation of benzylic proton with the formation of H_2O_2 . Noteworthily, the accompanied product H_2O_2 was detected using UV-visible spectroscopy.

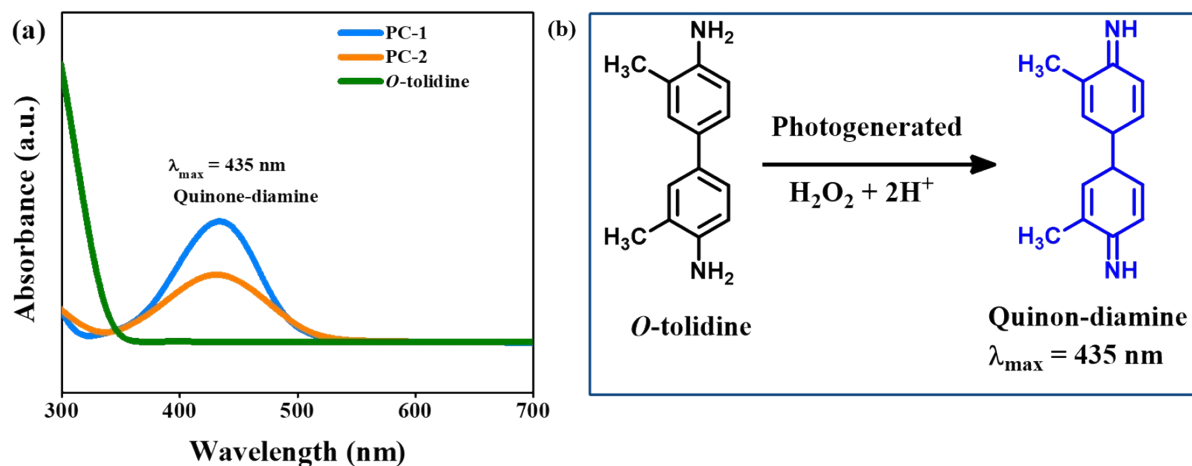
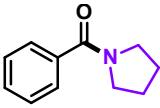
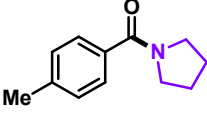
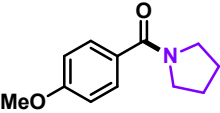
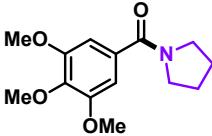
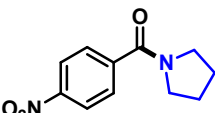
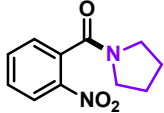
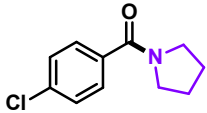
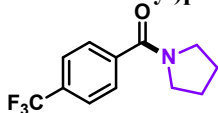
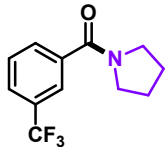
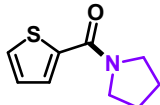
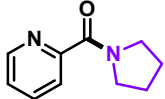
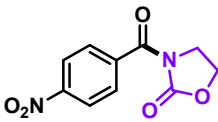
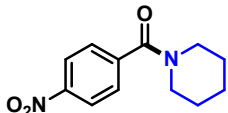
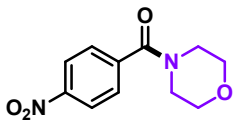
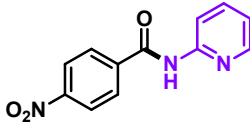


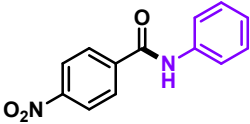
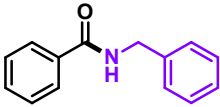
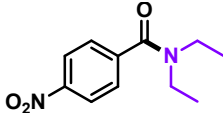
Figure S17. (a) UV-visible spectroscopic detection of photogenerated H_2O_2 in the reaction mixture. (b) Oxidation of *o*-tolidine with H_2O_2 forms blue-colored quinone-diamine ($\lambda_{\text{max}} = 435 \text{ nm}$).⁴

Reaction conditions: After amide bond formation reaction, PC-1 was separated by centrifugation at 12000 rpm/minute for 5 minutes. In addition, photogenerated hydrogen peroxide was separated (by separating funnel) in water (2 mL) from the reaction mixture. Further, 10 μL aliquot was taken and added to the *o*-tolidine solution (1 wt. % of *o*-tolidine in 0.1 M HCl), and UV-visible spectra were recorded.

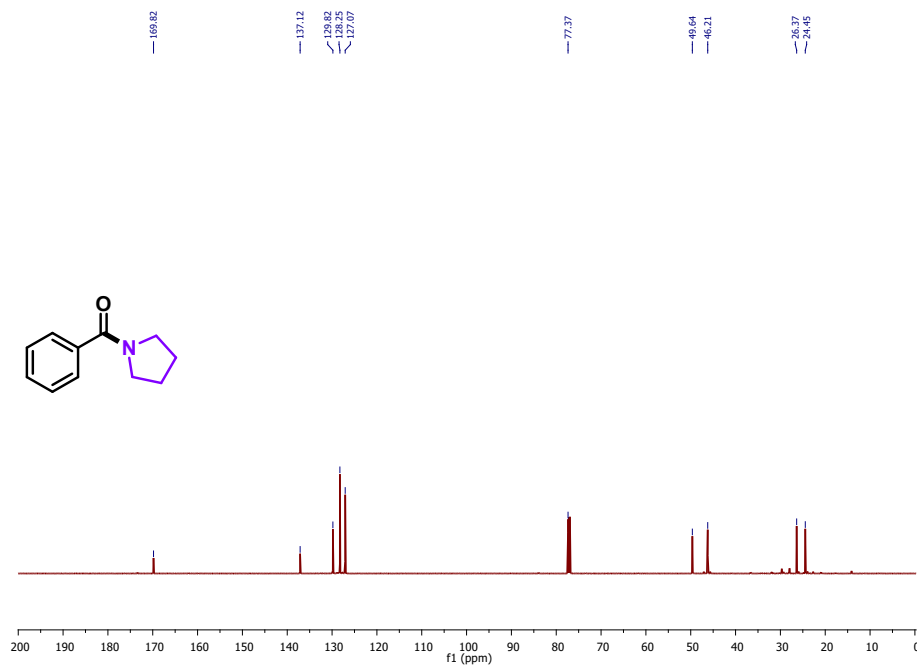
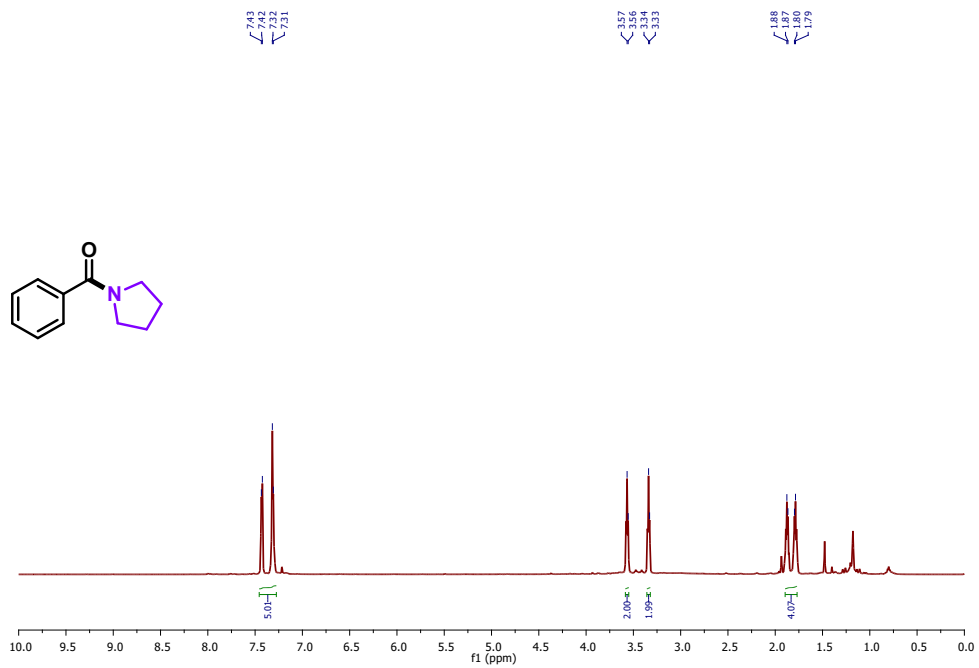
Table S3. ^1H NMR and ^{13}C NMR spectra of the products.^{5,6,7}

<p>3a. phenyl(pyrrolidin-1-yl)methanone</p> 	<p>^1H NMR (500 MHz, CDCl_3) δ: 7.37 (dd, J = 69.7, 6.3 Hz, 5H), 3.56 (d, 2H), 3.33 (d, 2H), 1.83 (dt, 4H). ^{13}C NMR (126 MHz, CDCl_3) δ: 169.82, 137.12, 129.82, 128.25, 127.07, 49.64, 46.21, 26.37, 24.45.</p> <p>Yield: 88% (77 mg and 0.44 mmol)</p>
<p>3b. pyrrolidin-1-yl(p-tolyl)methanone</p> 	<p>^1H NMR (500 MHz, CDCl_3) δ: 7.43 (d, J = 8.1 Hz, 2H), 7.20 (d, J = 7.9 Hz, 2H), 3.64 (d, 2H), 3.44 (d, 2H), 2.38 (s, 3H), 1.91 (dt, 4H). ^{13}C NMR (126 MHz, CDCl_3) δ: 169.92, 139.96, 134.19, 128.83, 127.22, 49.71, 46.25, 26.41, 24.46, 21.40.</p> <p>Yield: 84% (80 mg and 0.42 mmol)</p>
<p>3c. (4-methoxyphenyl)(pyrrolidin-1-yl)methanone</p> 	<p>^1H NMR (500 MHz, CDCl_3) δ: 7.49 (d, J = 7.2 Hz, 2H), 6.87 (d, J = 7.2 Hz, 2H), 3.80 (s, 3H), 3.60 (dd, 2H), 3.45 (dd, 2H), 1.88 (dt, 4H). ^{13}C NMR (126 MHz, CDCl_3) δ: 169.45, 160.78, 129.41, 129.23, 113.35, 55.23, 49.79, 46.33, 26.47, 24.42.</p> <p>Yield: 83% (80 mg and 0.41 mmol)</p>
<p>3d. pyrrolidin-1-yl(3,4,5-trimethoxyphenyl)methanone</p> 	<p>^1H NMR (500 MHz, CDCl_3) δ: 7.34 (d, J = 51.5 Hz, 2H), 3.95 (s, 9H), 3.89 (dd, 2H), 3.88 (dd, 2H) 1.52 (dt, 4H). ^{13}C NMR (126 MHz, CDCl_3) δ: 170.63, 152.97, 142.82, 124.32, 107.38, 61.04, 56.17, 29.71, 22.70.</p> <p>Yield: 80% (106 mg and 0.40 mmol)</p>
<p>3e. (4-nitrophenyl)(pyrrolidin-1-yl)methanone</p> 	<p>^1H NMR (500 MHz, CDCl_3) δ: 8.24 (d, J = 8.8 Hz, 2H), 7.66 (d, J = 8.8 Hz, 2H), 3.64 (t, 2H), 3.36 (t, 2H), 1.93 (dt, 4H). ^{13}C NMR (126 MHz, CDCl_3) δ: 167.52, 148.47, 143.11, 128.18, 123.80, 49.54, 46.48, 26.43, 24.42.</p> <p>Yield: 97% (107 mg and 0.48 mmol)</p>
<p>3f. (2-nitrophenyl)(pyrrolidin-1-yl)methanone</p> 	<p>^1H NMR (500 MHz, CDCl_3) δ: 8.17 (d, J = 9.2 Hz, 1H), 7.71 (t, J = 8.1 Hz, 1H), 7.58 – 7.53 (m, 1H), 7.44 (d, J = 6.3 Hz, 1H), 3.70 (t, 2H), 3.15 (t, 2H), 1.95 (dt, 4H). ^{13}C NMR (126 MHz, CDCl_3) δ: 171.16, 166.18, 144.94, 134.02, 129.76, 128.18, 124.70, 48.22, 45.82, 25.81, 24.50.</p> <p>Yield: 91% (101 mg and 0.46 mmol)</p>
<p>3g. (4-chlorophenyl)(pyrrolidin-1-yl)methanone</p> 	<p>^1H NMR (500 MHz, CDCl_3) δ: 7.47 (d, J = 8.3 Hz, 2H), 7.38 (d, J = 8.4 Hz, 2H), 3.63 (d, 2H), 3.41 (d, 2H), 1.93 (dd, 4H). ^{13}C NMR (126 MHz, CDCl_3) δ: 168.68, 135.89, 135.39, 128.67, 128.53, 49.67, 46.36, 26.41, 24.41.</p> <p>Yield: 95% (99 mg and 0.47 mmol)</p>
<p>3h. pyrrolidin-1-yl(4-</p>	<p>^1H NMR (500 MHz, CDCl_3) δ: 7.57 (d, J = 8.2 Hz, 4H), 3.57 (t, 2H), 3.30 (t, 2H), 1.84 (dt, 4H).</p>

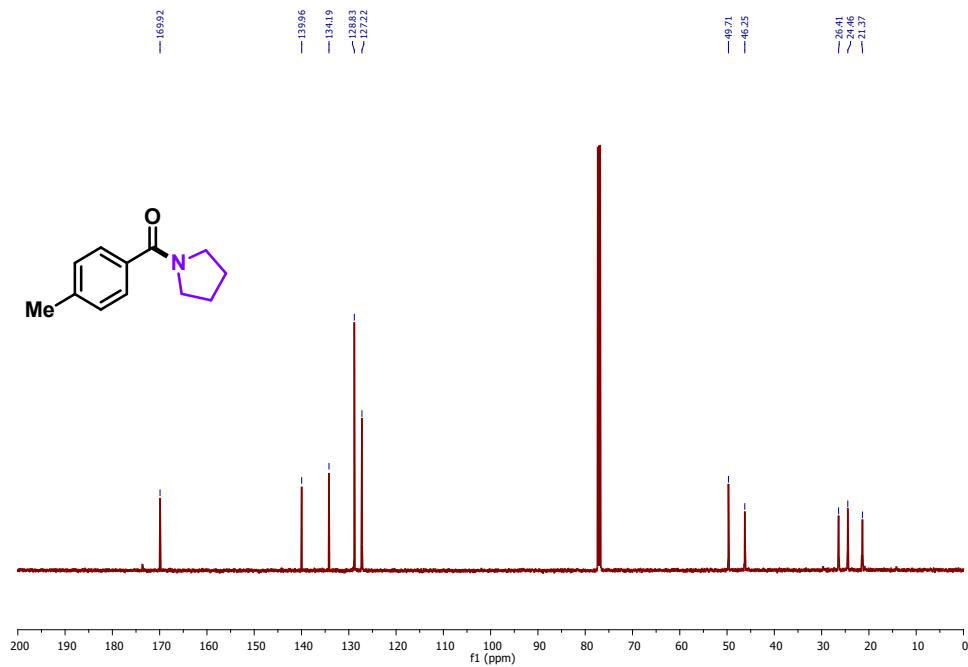
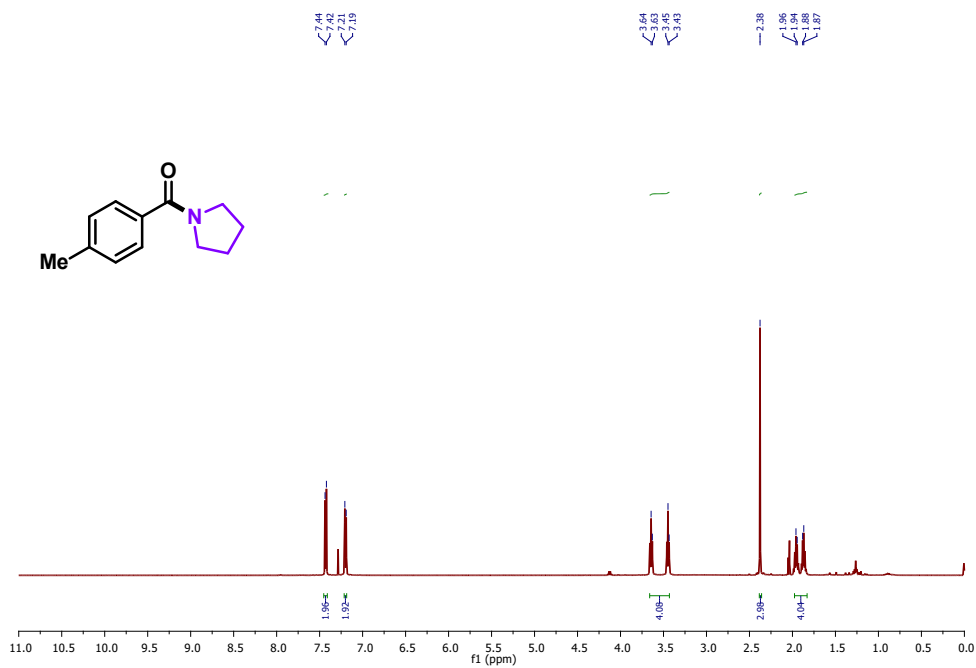
<p>(trifluoromethyl)phenyl)methanone</p> 	<p>^{13}C NMR (126 MHz, CDCl_3) δ 168.11, 140.67, 131.57, 127.39, 125.02, 122.64, 49.36, 46.15, 26.22, 24.25.</p> <p>Yield: 98% (120 mg and 0.49 mmol)</p>
<p>3i. pyrrolidin-1-yl(2-(trifluoromethyl)phenyl)methanone</p> 	<p>^1H NMR (500 MHz, CDCl_3) δ: 7.82 (s, 1H), 7.74 (d, J = 7.7 Hz, 1H), 7.69 (d, J = 7.9 Hz, 1H), 7.58 – 7.55 (m, 1H), 3.70 (t, 2H), 3.44 (t, 2H), 1.96 (dt, 4H).</p> <p>^{13}C NMR (126 MHz, CDCl_3) δ: 168.80, 153.34, 151.99, 126.50, 121.04, 116.66, 113.97, 111.75, 47.83, 25.18.</p> <p>Yield: 83% (100 mg and 0.41 mmol)</p>
<p>3j. pyrrolidin-1-yl(thiophen-2-yl)methanone</p> 	<p>^1H NMR (500 MHz, CDCl_3) δ: 7.54 (d, J = 3.7 Hz, 1H), 7.49 (d, J = 5.0 Hz, 1H), 7.09 (t, 1H), 3.73 (dt, 4H), 1.99 (dd, 4H).</p> <p>^{13}C NMR (126 MHz, CDCl_3) δ: 161.90, 139.45, 129.63, 127.13, 48.98, 47.39, 26.74, 24.10.</p> <p>Yield: 82% (74 mg and 0.41 mmol)</p>
<p>3k. pyridin-2-yl(pyrrolidin-1-yl)methanone</p> 	<p>^1H NMR (500 MHz, CDCl_3) δ: 8.51 (s, 1H), 7.73 (d, J = 6.7 Hz, 2H), 7.28 (s, 1H), 3.63 (dd, 4H), 1.85 (dd, 4H).</p> <p>^{13}C NMR (126 MHz, CDCl_3) δ: 166.52, 154.39, 147.97, 136.83, 124.68, 123.67, 49.05, 46.78, 26.51, 23.98.</p> <p>Yield: 84% (74 mg and 0.42 mmol)</p>
<p>3l. 3-(4-nitrobenzoyl)oxazolidin-2-one</p> 	<p>^1H NMR (500 MHz, DMSO) δ: 8.33 (d, J = 8.9 Hz, 1H), 8.18 (d, J = 9.0 Hz, 1H), 3.36 (s, 2H).</p> <p>^{13}C NMR (126 MHz, DMSO) δ: 172.67, 157.68, 147.83, 140.52, 128.97, 124.40, 64.76, 41.84.</p> <p>Yield: 78% (92 mg and 0.39 mmol)</p>
<p>3m. (4-nitrophenyl)(piperidin-1-yl)methanone</p> 	<p>^1H NMR (500 MHz, CDCl_3) δ: 8.28 (d, J = 8.8 Hz, 2H), 7.57 (d, J = 8.8 Hz, 2H), 3.51 (d, 4H), 1.62 (d, 6H).</p> <p>^{13}C NMR (126 MHz, CDCl_3) δ: 167.95, 148.18, 142.66, 127.79, 123.90, 48.67, 43.23, 26.51, 25.50, 24.39.</p> <p>Yield: 88% (111 mg and 0.47 mmol)</p>
<p>3n. morpholino(4-nitrophenyl)methanone</p> 	<p>^1H NMR (500 MHz, CDCl_3) δ: 8.30 (d, J = 8.8 Hz, 2H), 7.60 (d, J = 8.8 Hz, 2H), 3.75 (dd, 4H).</p> <p>^{13}C NMR (126 MHz, CDCl_3) δ: 168.13, 148.50, 141.38, 128.14, 123.96, 66.73, 48.06.</p> <p>Yield: 79% (93 mg and 0.39 mmol)</p>
<p>3o. 4-nitro-N-(pyridin-2-yl)benzamide</p> 	<p>^1H NMR (500 MHz, DMSO) δ: 11.19 (s, 1H), 8.41 (s, 1H), 8.34 (d, J = 8.9 Hz, 2H), 8.23 (d, J = 8.9 Hz, 3H), 7.88 (s, 1H), 7.21 (s, 1H).</p> <p>^{13}C NMR (126 MHz, DMSO) δ: 165.07, 152.30, 149.77, 148.48, 140.35, 138.68, 130.12, 123.81, 120.73, 115.37.</p> <p>Yield: 76% (92 mg and 0.38 mmol)</p>

<p>3p. 4-nitro-N-phenylbenzamide</p> 	<p>$^1\text{H NMR}$ (500 MHz, CDCl_3) δ: 8.58 (s, 1H), 8.37 (dd, $J = 12.2, 8.7$ Hz, 2H), 8.09 (dd, $J = 8.8, 3.5$ Hz, 2H), 7.44 (d, $J = 7.5$ Hz, 2H), 7.29 (dd, $J = 11.1, 9.9$ Hz, 3H). $^{13}\text{C NMR}$ (126 MHz, CDCl_3) δ: 169.42, 150.93, 141.59, 140.06, 130.46, 129.36, 127.10, 124.00, 120.99.</p> <p>Yield: 74% (90 mg and 0.37 mmol)</p>
<p>3q. N-benzylbenzamide</p> 	<p>$^1\text{H NMR}$ (500 MHz, CDCl_3) δ 7.82 (d, $J = 7.1$ Hz, 2H), 7.52 (t, $J = 7.4$ Hz, 1H), 7.45 (t, $J = 7.5$ Hz, 2H), 7.38 (d, $J = 4.4$ Hz, 4H), 7.33 (d, $J = 4.4$ Hz, 1H), 6.53 (s, 1H), 4.67 (d, $J = 5.7$ Hz, 2H). $^{13}\text{C NMR}$ (126 MHz, CDCl_3) δ 167.41, 138.20, 134.40, 131.59, 128.81, 128.62, 127.94, 127.65, 127.03, 126.99, 44.16.</p> <p>Yield: 71% (62 mg and 0.35 mmol)</p>
<p>3r. N,N-diethyl-4-nitrobenzamide</p> 	<p>$^1\text{H NMR}$ (500 MHz, CDCl_3) δ 8.36 (d, $J = 8.92$ Hz, 2H), 8.13 (d, $J = 8.7$ Hz, 2H), 3.45 (q, 2H), 3.27 (q, 2H), 1.27 (t, 6H). $^{13}\text{C NMR}$ (126 MHz, CDCl_3) δ 171.31, 140.02, 137.32, 129.07, 128.38, 126.28, 43.29, 39.34, 14.15, 13.00.</p> <p>Yield: 66% (73 mg and 0.32 mmol)</p>

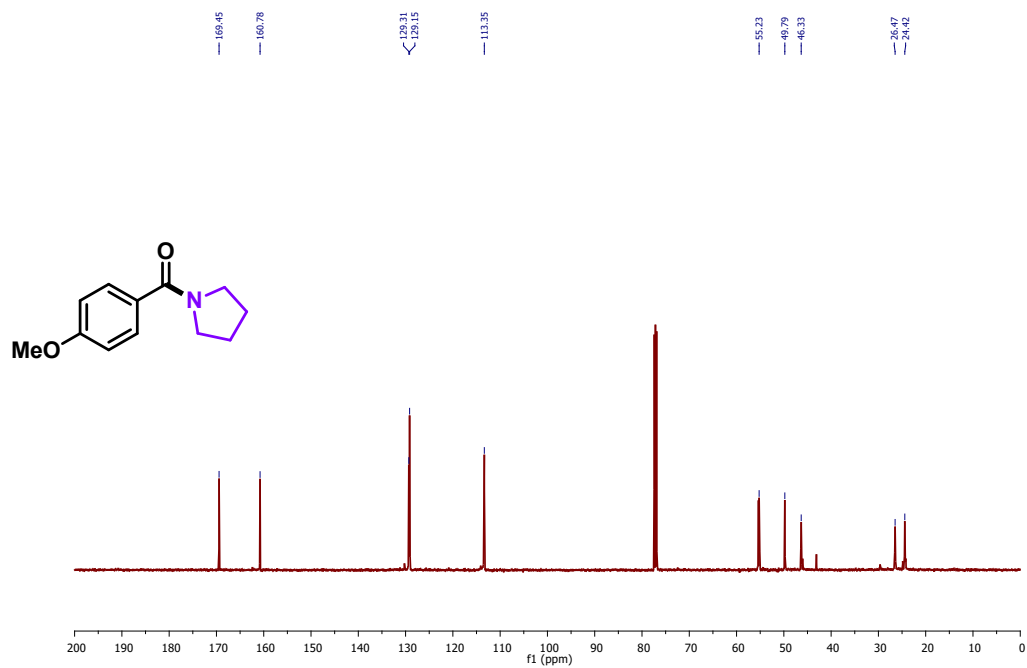
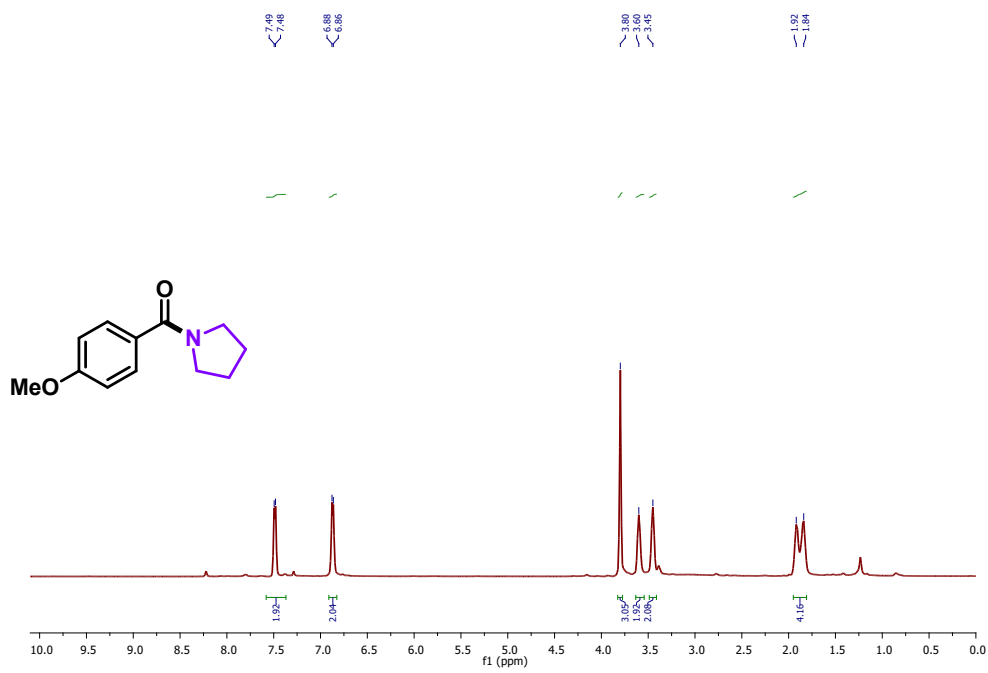
$^1\text{H NMR}$ and $^{13}\text{C NMR}$ spectra of product 3a.



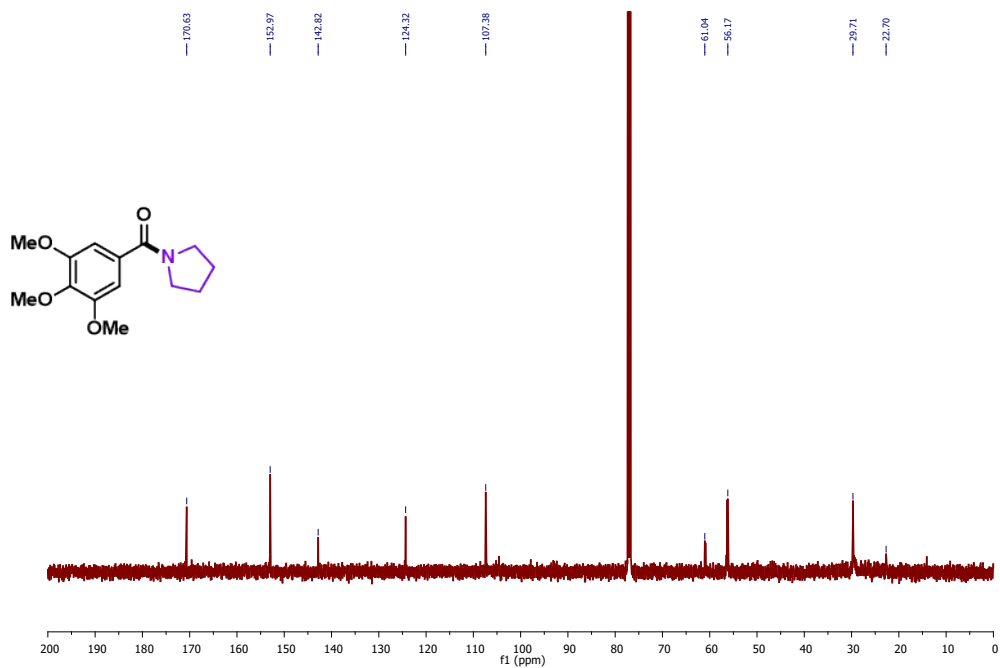
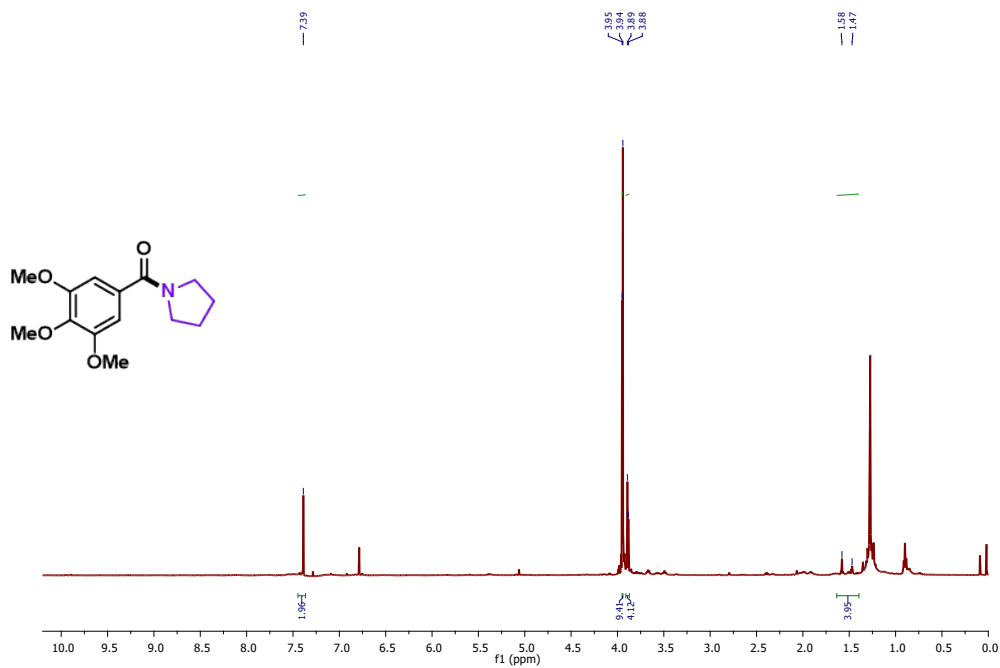
^1H NMR and ^{13}C NMR spectra of product 3b.



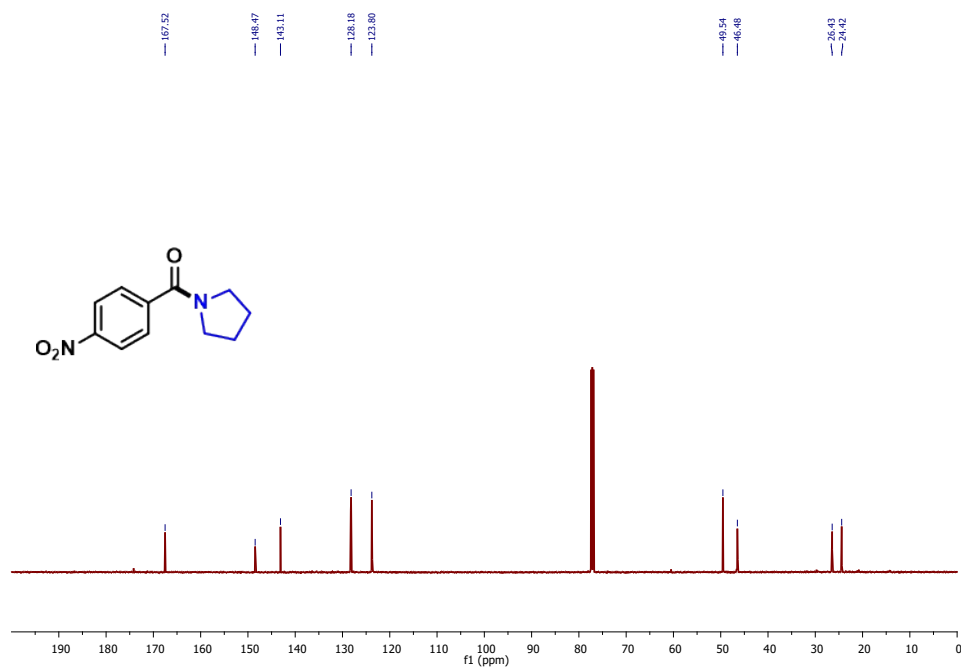
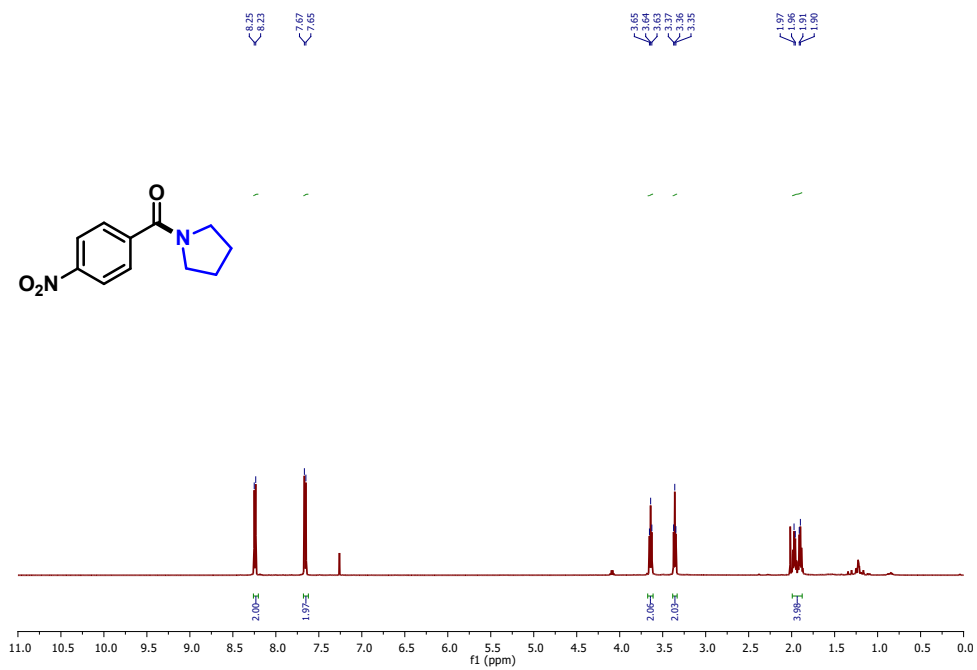
¹H NMR and ¹³C NMR spectra of product 3c.



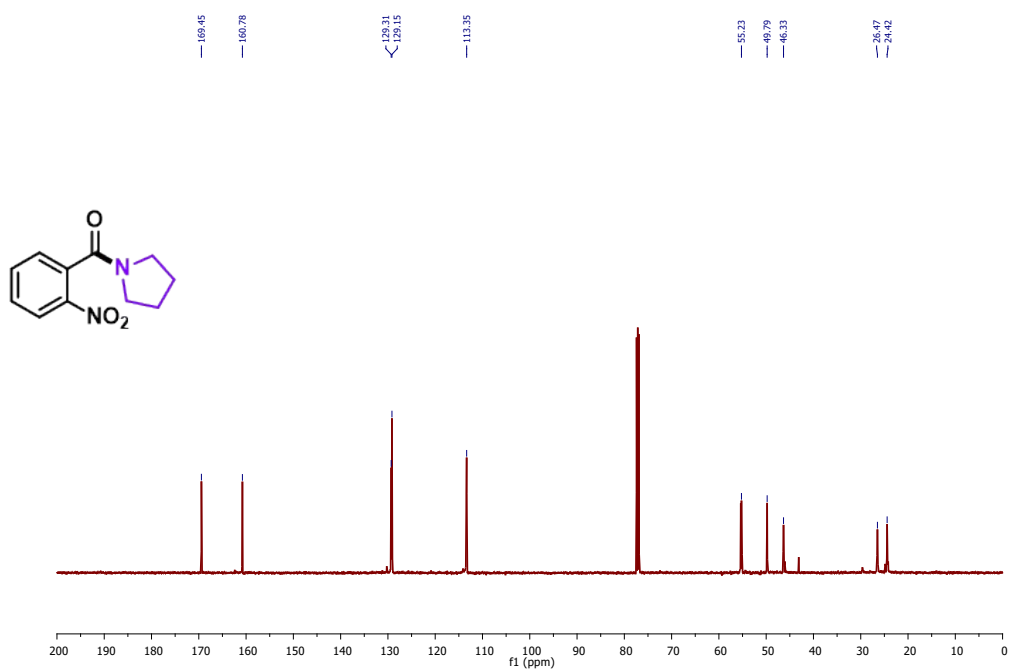
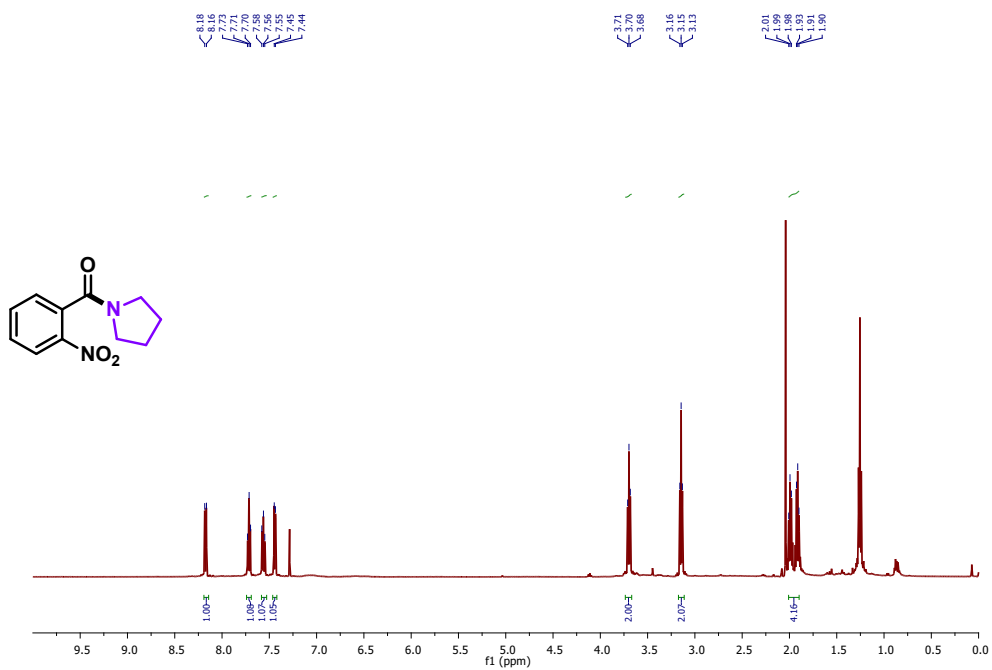
¹H NMR and ¹³C NMR spectra of product 3d.



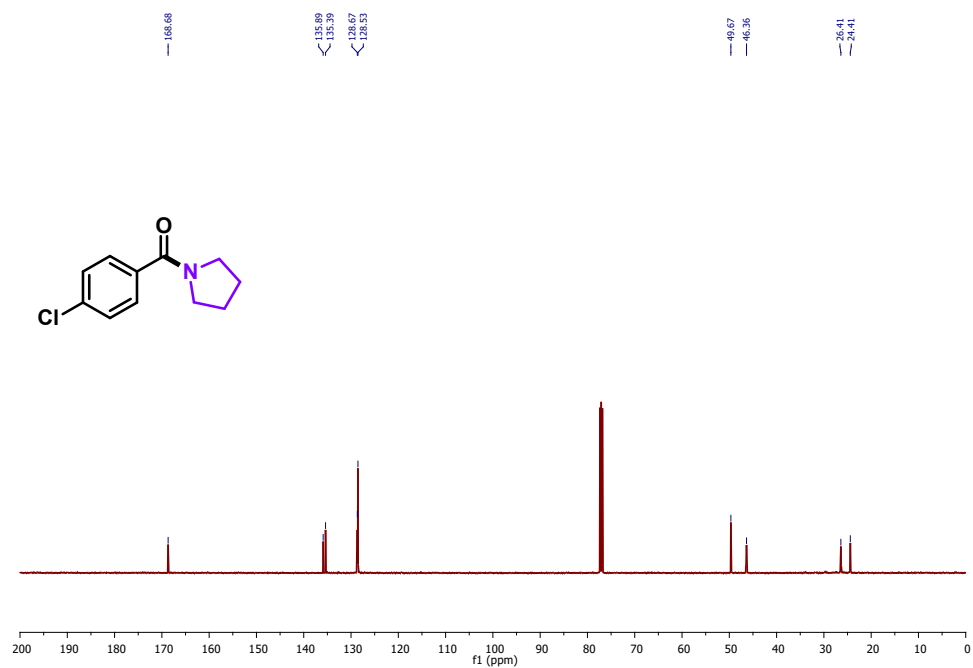
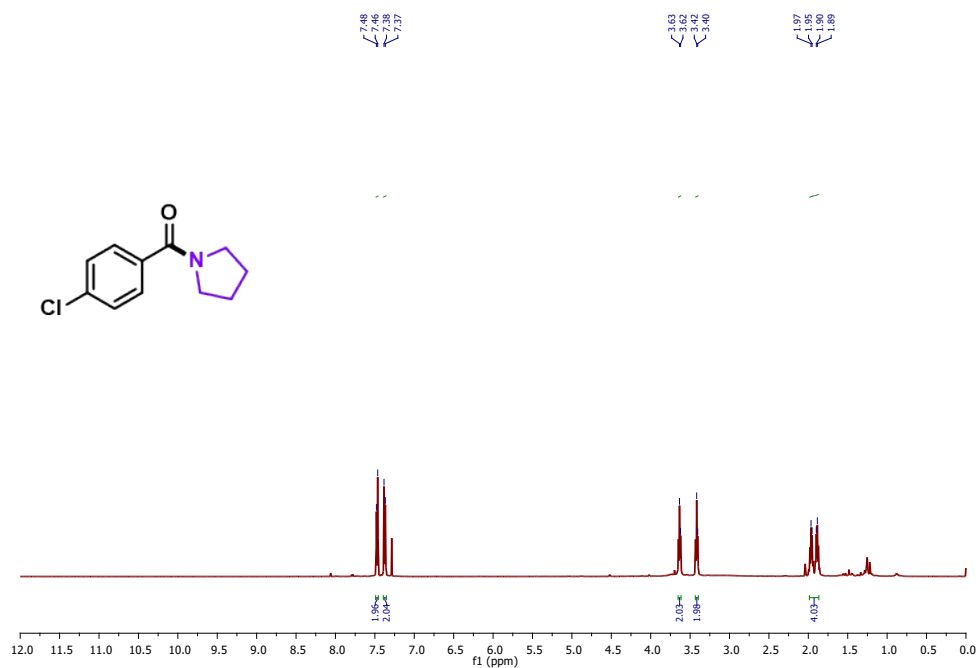
¹H NMR and ¹³C NMR spectra of product 3e.



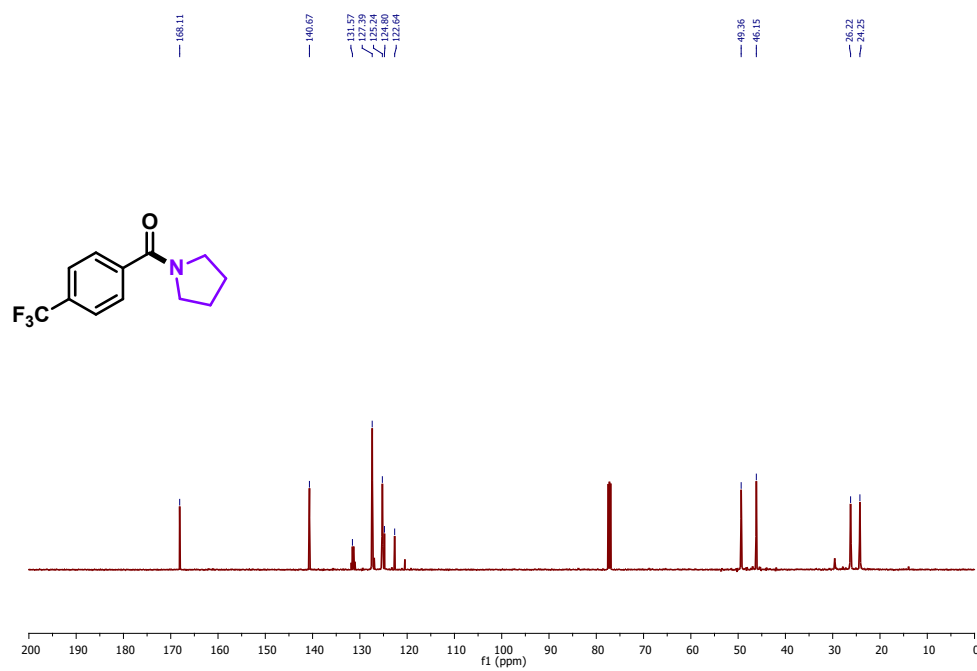
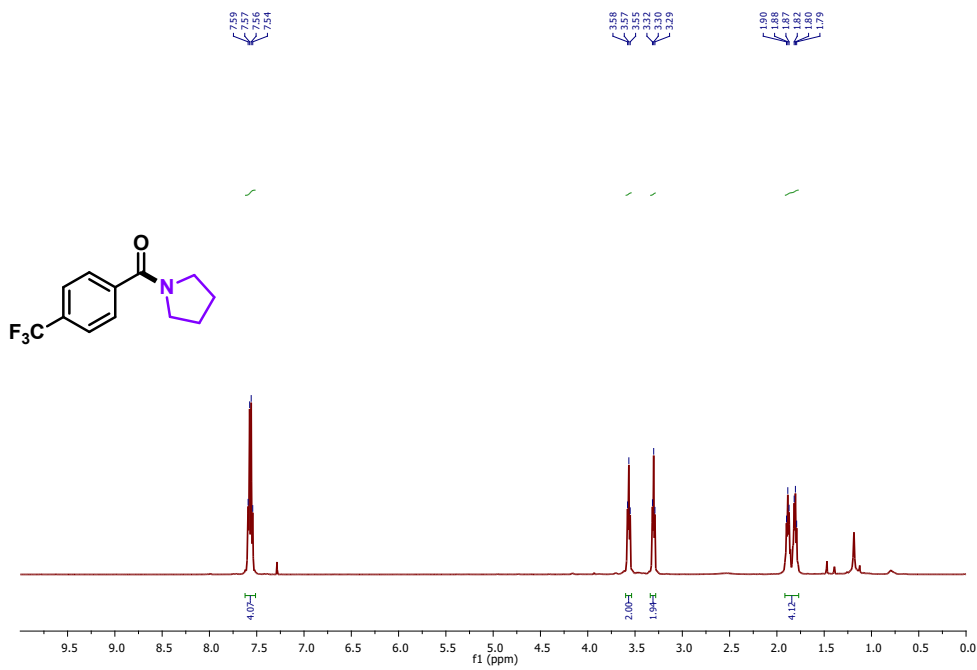
^1H NMR and ^{13}C NMR spectra of product 3f.



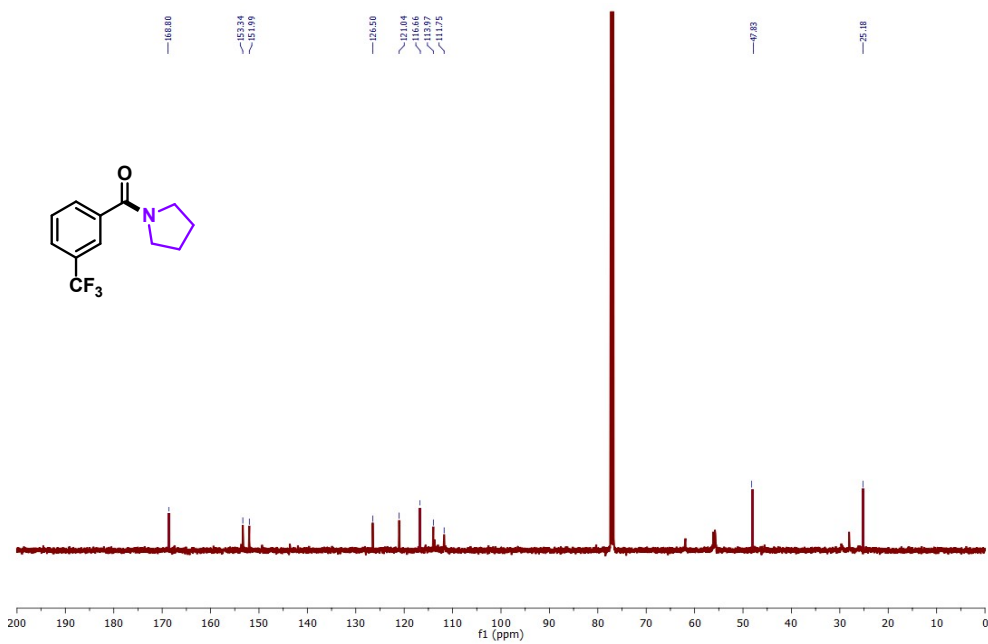
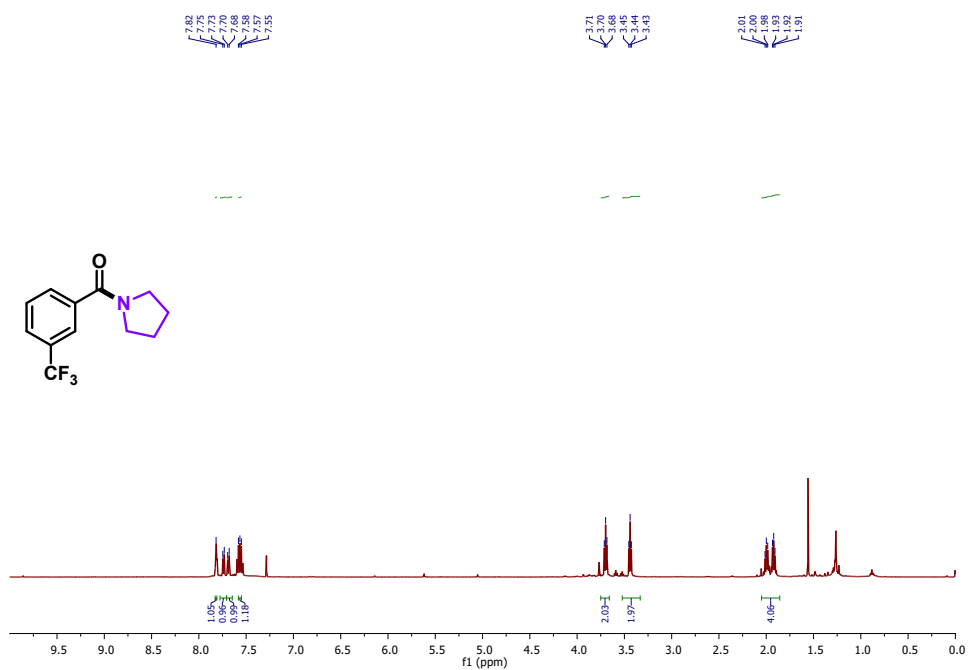
¹H NMR and ¹³C NMR spectra of product 3g.



^1H NMR and ^{13}C NMR spectra of product 3h.

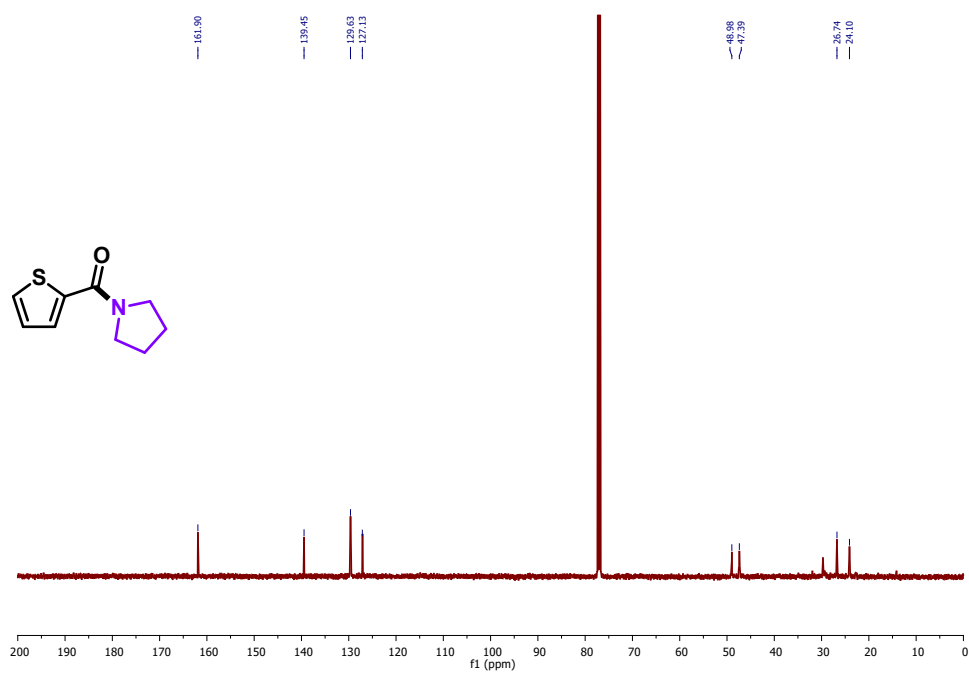


¹H NMR and ¹³C NMR spectra of product 3i.

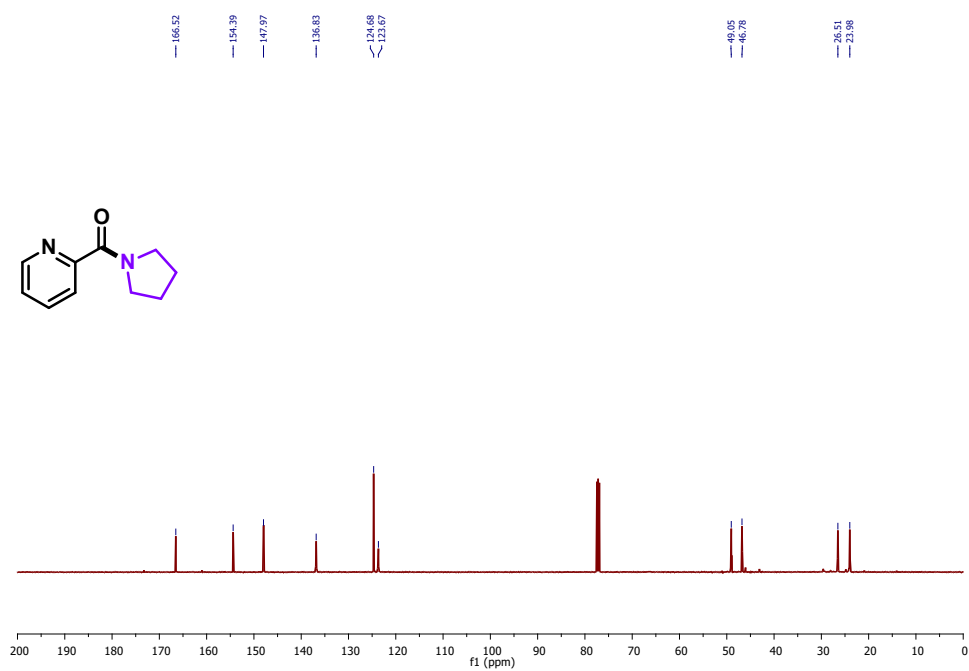
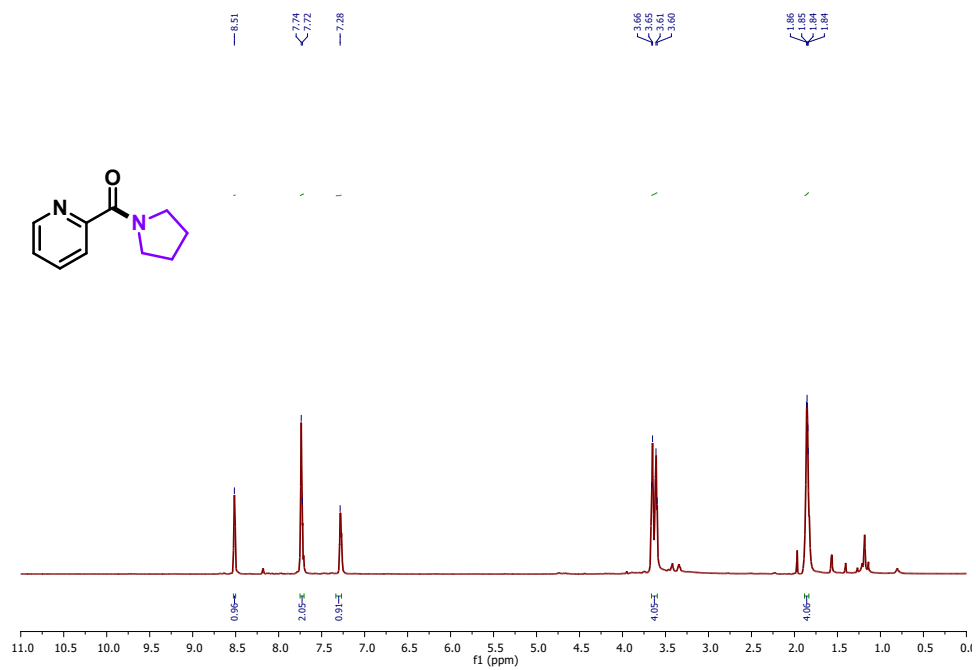


¹H NMR and ¹³C NMR spectra of product 3j.

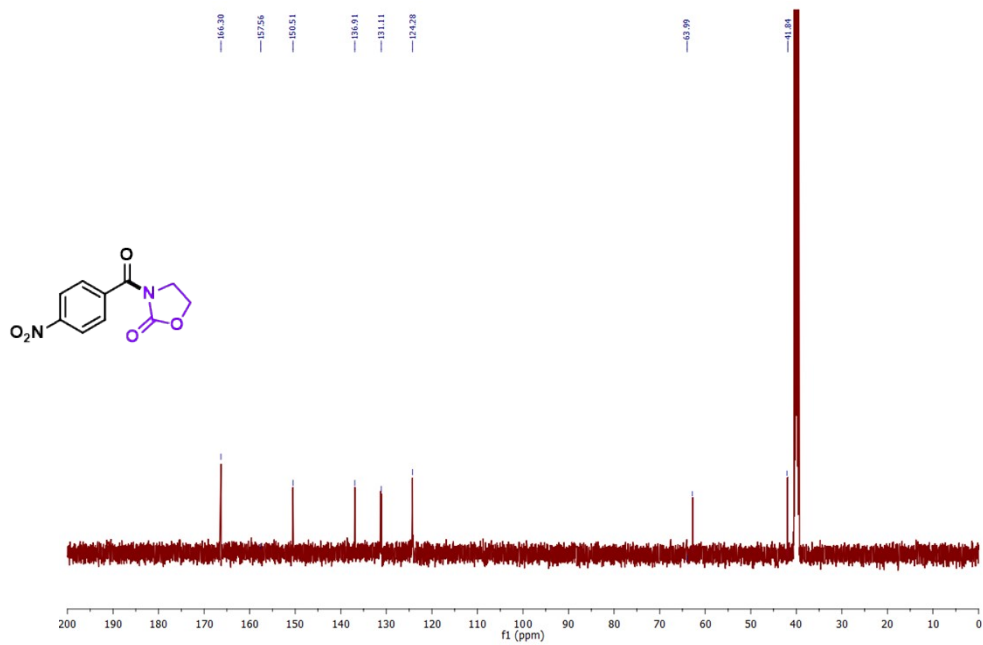
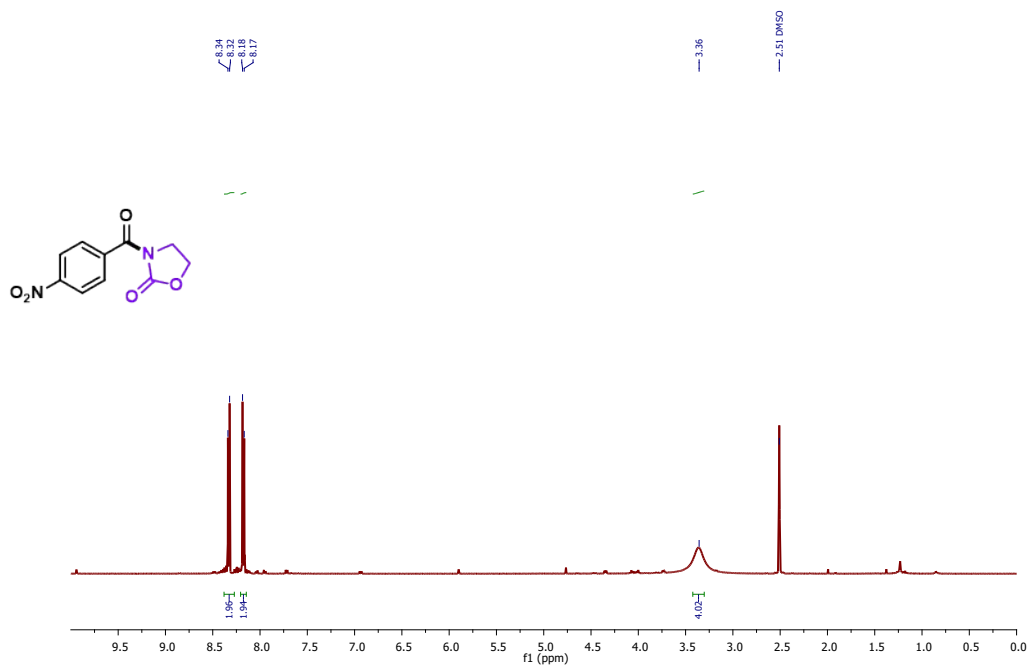




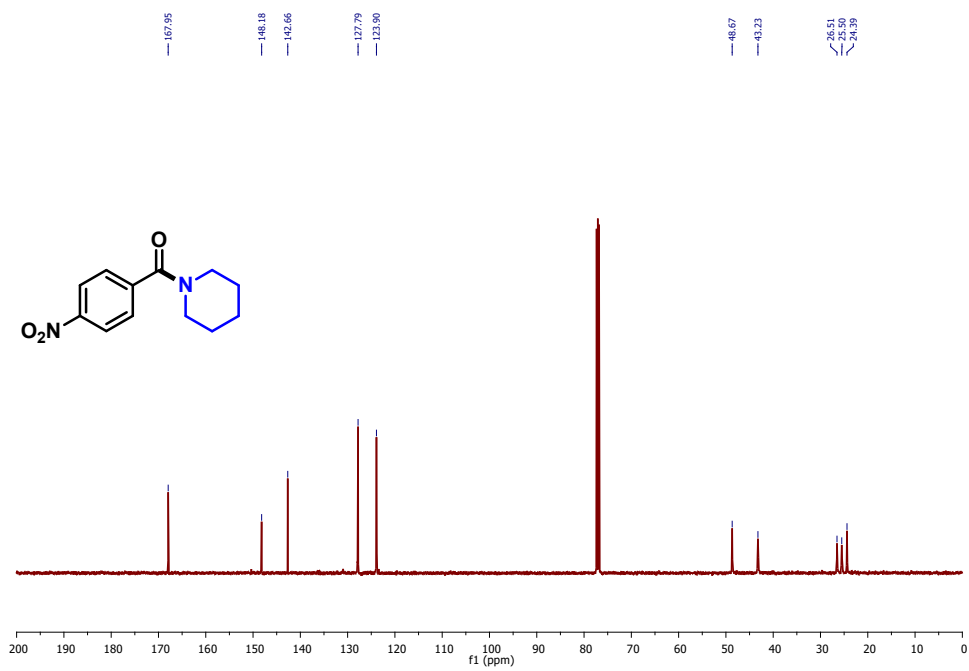
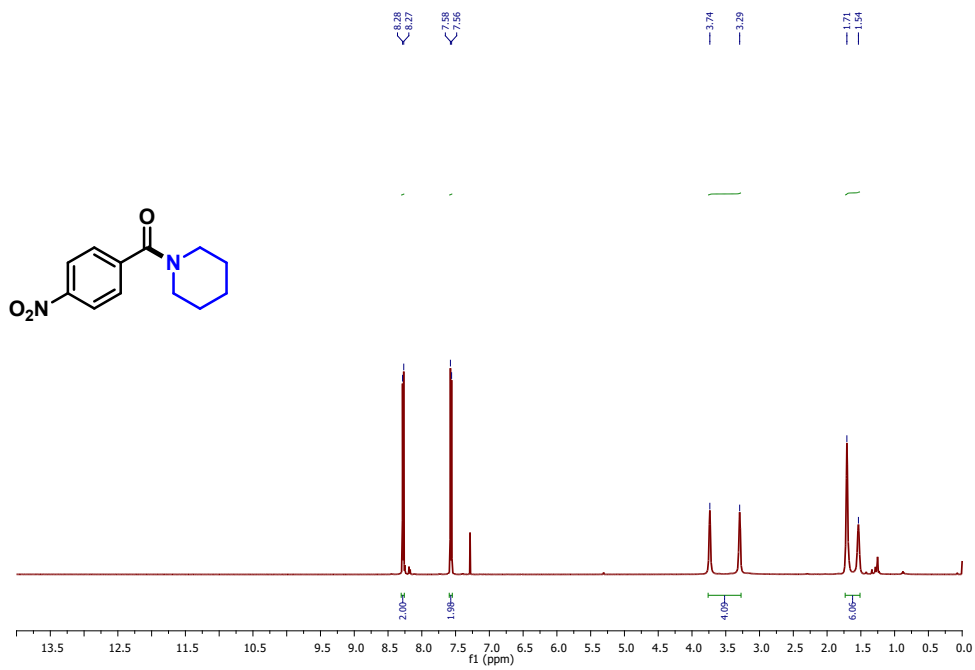
¹H NMR and ¹³C NMR spectra of product 3k.



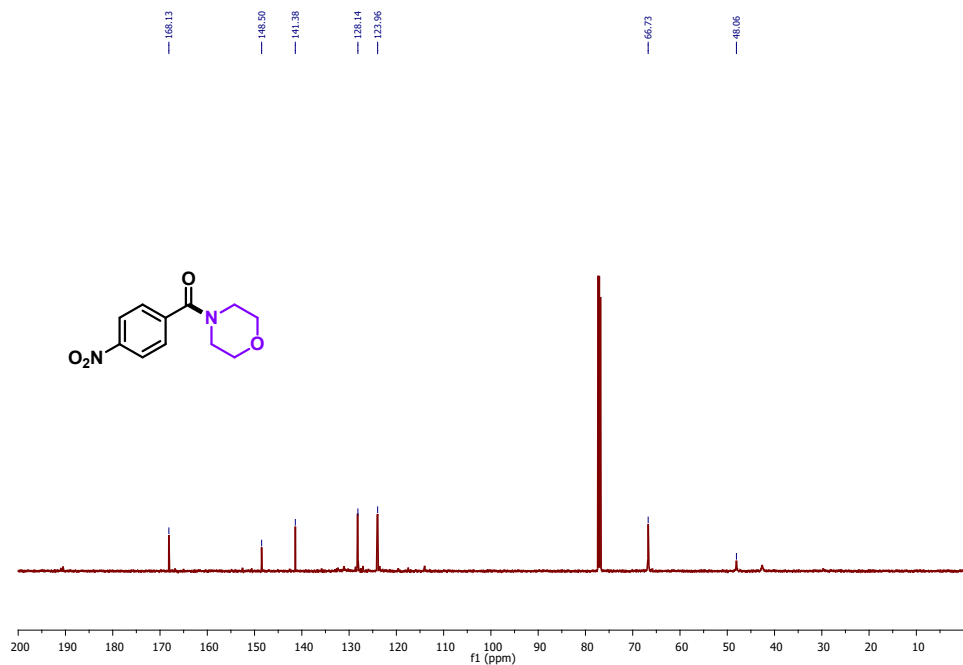
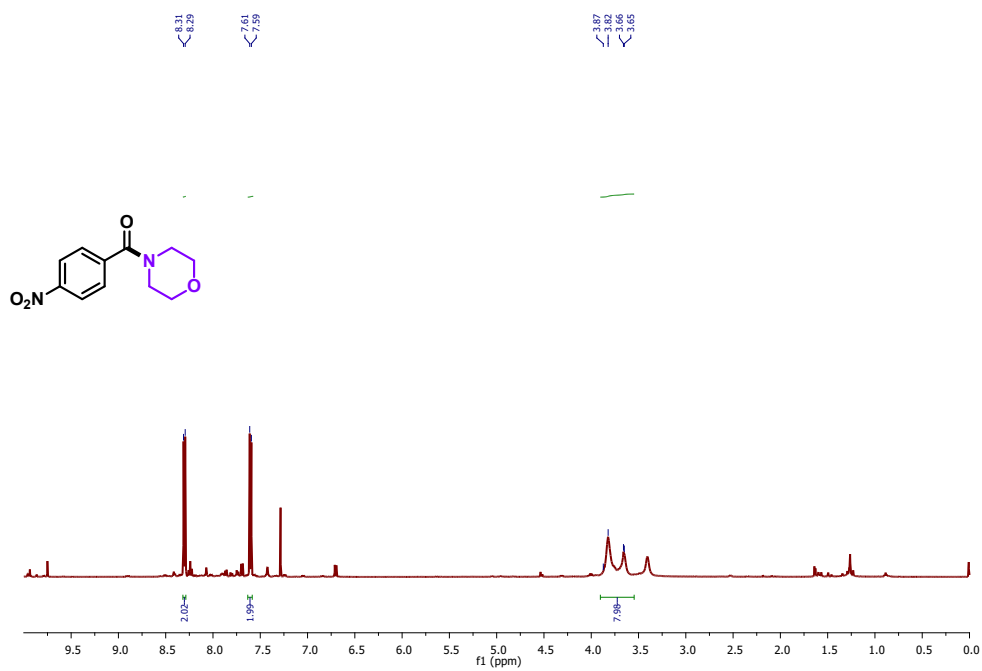
^1H NMR and ^{13}C NMR spectra of product 3l.



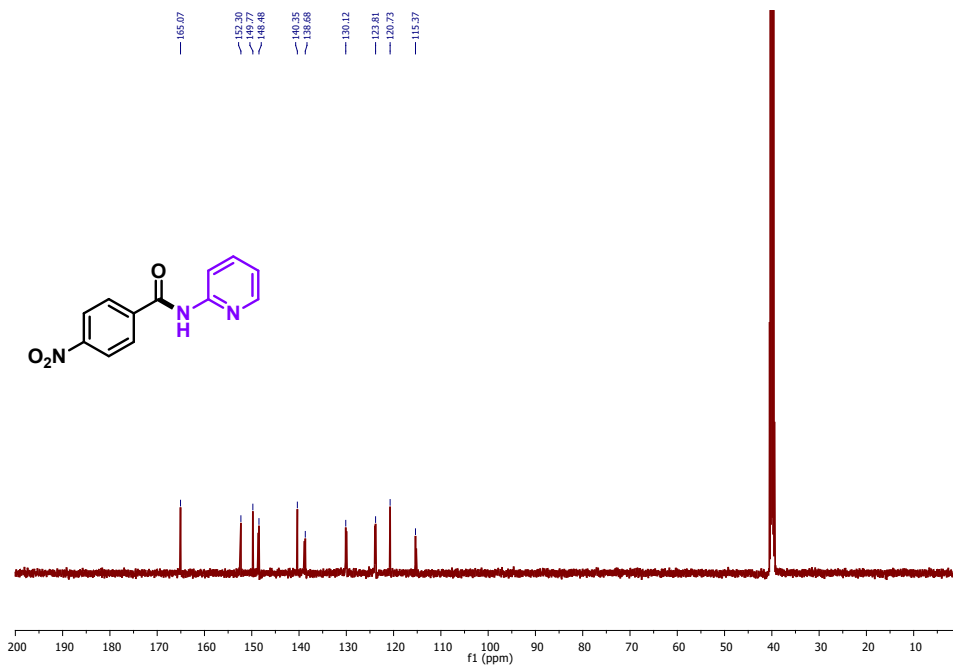
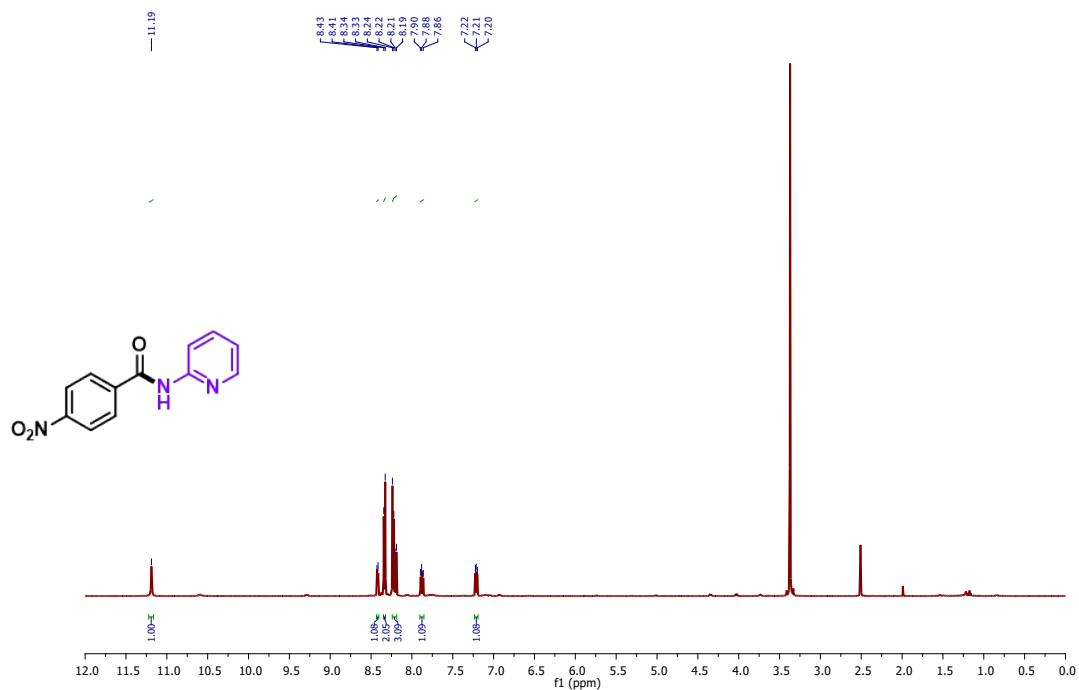
^1H NMR and ^{13}C NMR spectra of product 3m.



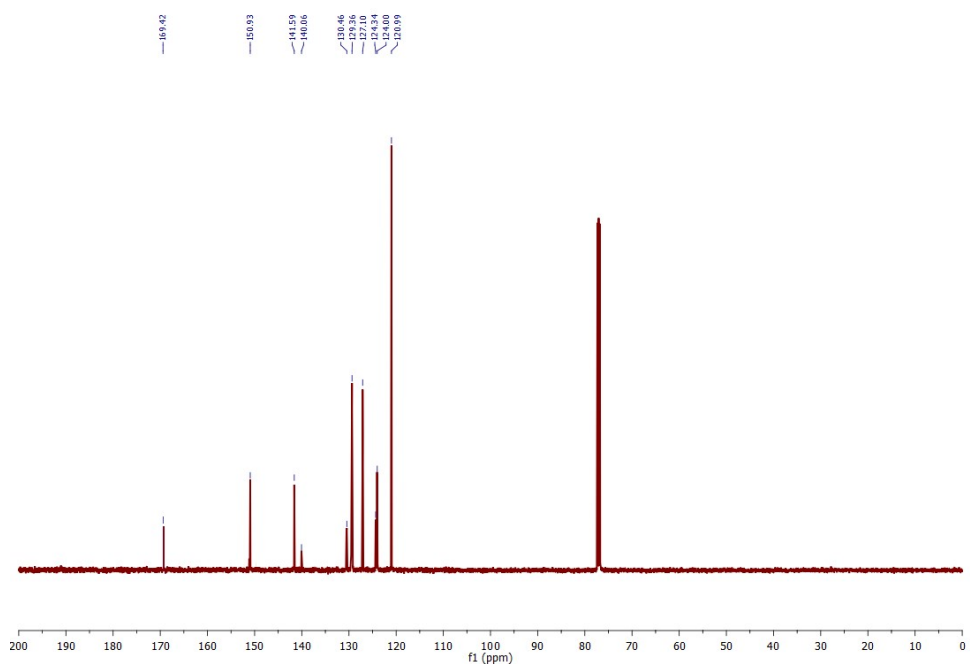
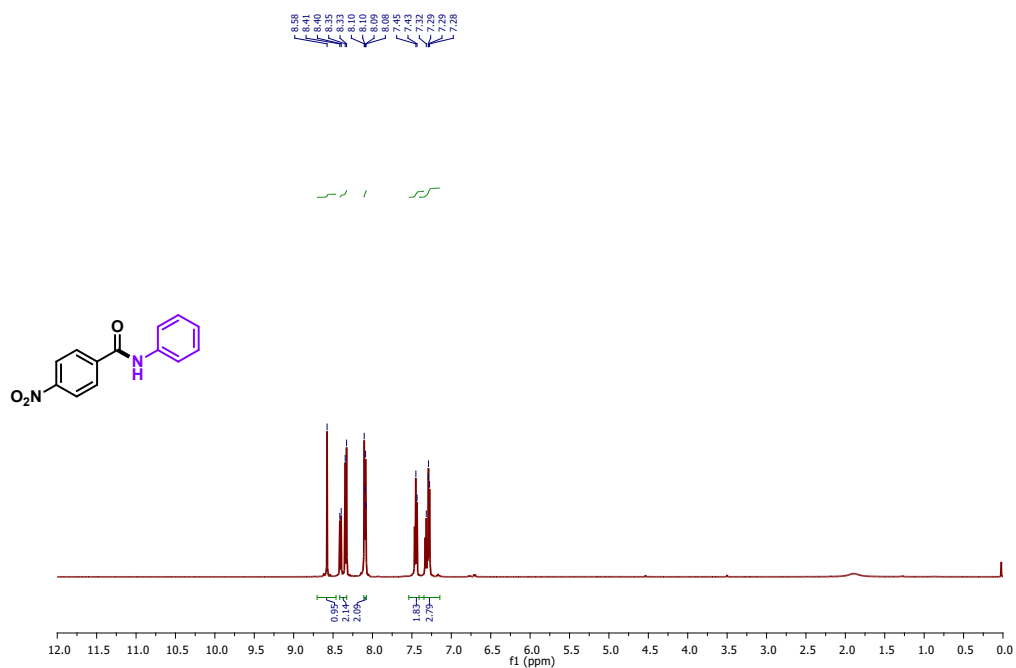
^1H NMR and ^{13}C NMR spectra of product 3n.



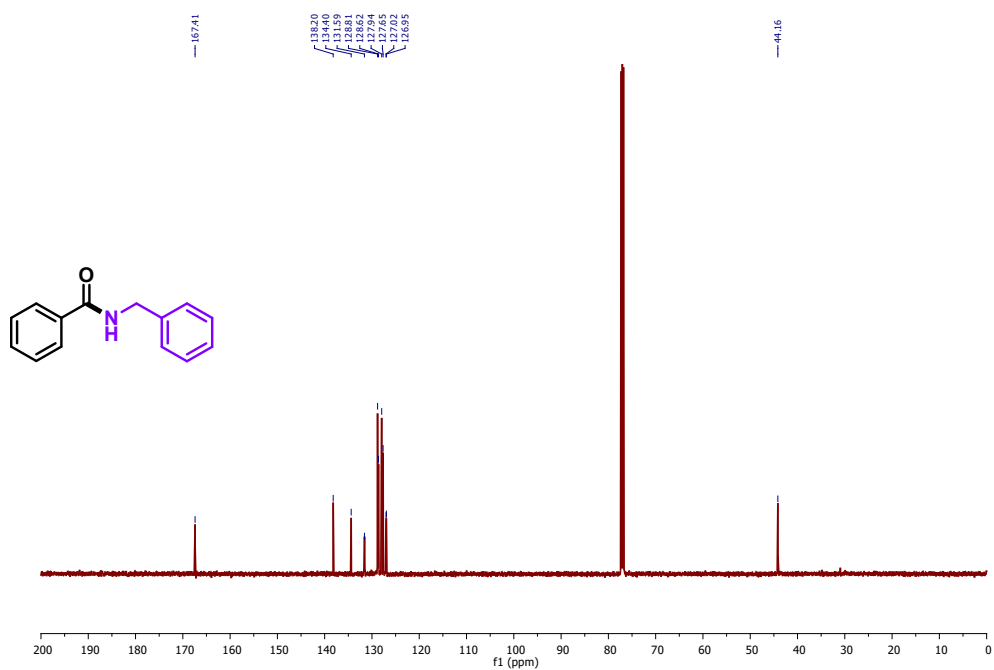
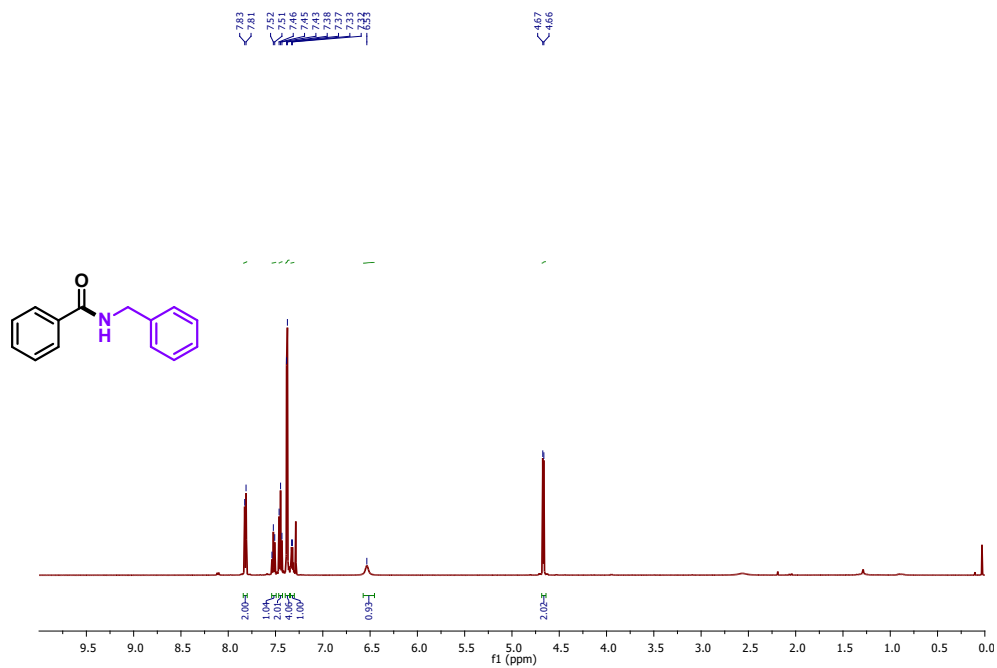
¹H NMR and ¹³C NMR spectra of product 3o.



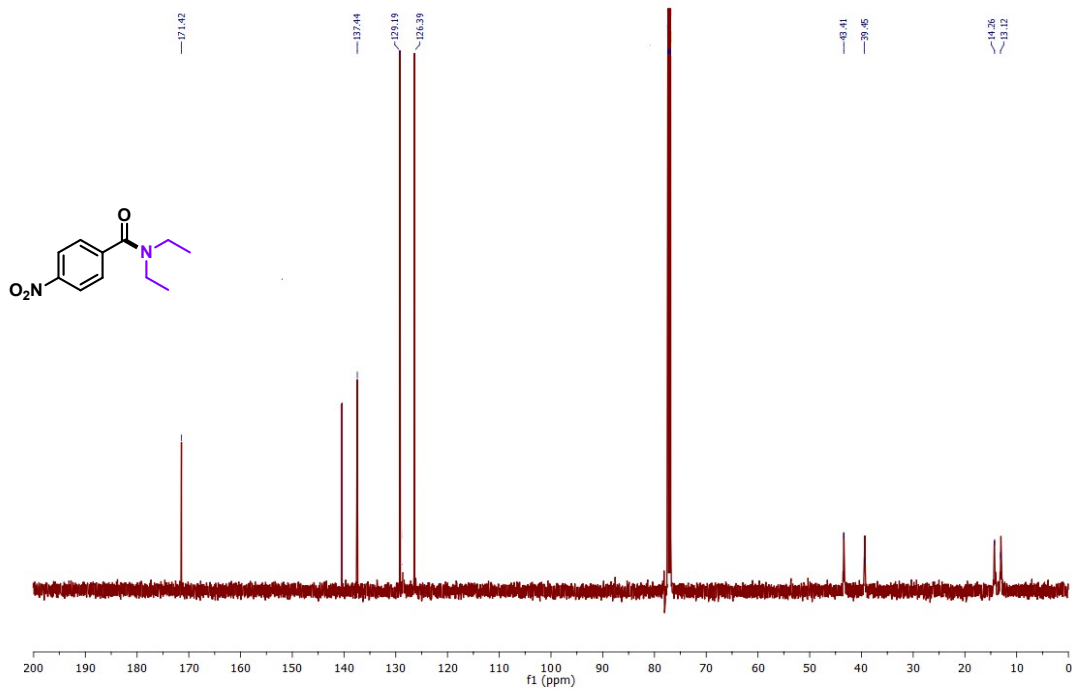
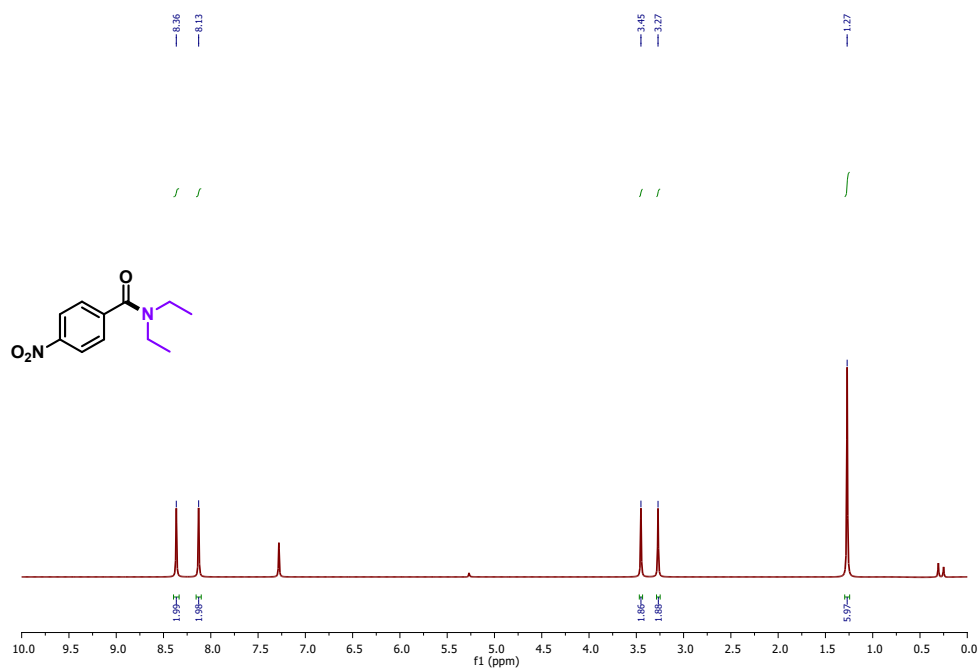
¹H NMR and ¹³C NMR spectra of product 3p.



^1H NMR and ^{13}C NMR spectra of product 3q.



^1H NMR and ^{13}C NMR spectra of product 3r.



References:

1. X. Zhu, Y. Lin, J. San Martin, Y. Sun, D. Zhu and Y. Yan, *Nat. Commun.*, 2019, **10**, 2843.
2. J. Sheng, Y. He, M. Huang, C. Yuan, S. Wang and F. Dong, *ACS Catal.*, 2022, **12**, 2915–2926.
3. J. Luo, X. Wei, Y. Qiao, C. Wu, L. Li, L. Chen, and J. Shi, J., *Adv. Mater.*, 2023, **35**, 2210110.
4. Y. Deng, W. Liu, R. Xu, R. Gao, N. Huang, Y. Zheng, Y. Huang, H. Li, X. Y. Kong and L. Ye, *Angew. Chem. Int. Ed.*, 2024, e202319216.
5. A. Hassan Tolba, M. Krupička, J. Chudoba and R. Cibulka, *Org. Lett.*, 2021, **23**, 6825–6830.
6. A. Dey, S. Chakraborty, A. Singh, F.A. Rahimi, S. Biswas, T. Mandal, and T. K. Maji, *Angew. Chem. Int Ed.*, 2024, e2024 202403093.
7. Z. Akrami, and M. Hosseini-Sarvari, *Europ. J. Org. Chem.*, 2022, e202200429.